Dissertation

Mechanisms of neuroprotection and repair following immune mediated tissue damage

submitted by

Michaela Tanja HAINDL, BSc MSc

for the Academic Degree of

Doctor of Medical Science

Dr.scient.med.

at the

Medical University of Graz

Department of Neurology

under the Supervision of

Assoz.-Prof. Sonja HOCHMEISTER

Priv.-Doz. Willibald WONISCH

Univ.-Prof. Franz FAZEKAS

28.05.2019

Statutory Declaration

I hereby declare that this thesis is my own original work and that I have fully acknowledged by name all of those individuals and organizations that have contributed to the research for this thesis. Due acknowledgement has been made in the text to all other material used. Throughout this thesis and in all related publications I followed the "Standards of Good Scientific Practice and Ombuds committee at the Medical University of Graz".

Disclosures

1. Part of this thesis has been published in Haindl MT, Köck U, Zeitelhofer-Adzemovic M, Fazekas F, Hochmeister S. The formation of a glial scar does not prohibit remyelination in an animal model of multiple sclerosis. Glia. Wiley.; 2019; 67(3): 467-481.

2. Part of this thesis has been published in Ücal M, Haindl MT, Adzemovic MZ, Strasser J, Theisl L, Zeitelhofer M, Fazekas F, Hochmeister S. Widespread cortical demyelination of both hemispheres can be induced by injection of pro-inflammatory cytokines via an implanted catheter in the cortex of MOG-immunized rats. Exp Neurol. Elsevier Inc.; 2017; 294: 32–44.

Please note, that part of this thesis is therefore an identical reproduction of parts of those papers (primarily the methods and results part).

3. Part of this thesis has been published in Haindl MT, Ücal M, Fazekas F, Hochmeister S. Overview of Promising Rat Models for Cortical Lesion Research- 2006 Until Now. J Neurol Neuromed; 2018; 3(5): 8-12

All co-authors have explicitly agreed to the use of the data in my thesis:

Sonja Hochmeister[1], Muammer Ücal[4], Ulrike Köck[2], Lisa Theisl[1], Johannes Strasser[1], Stefan Ropele[1], Franz Fazekas[1], Klaus Kraitsy[4], Milena Zeitelhofer-Adzemovic[3], Ute Schäfer[4], Manuel Zeitelhofer[5]

[1]Department of Neurology, Medical University of Graz, Graz, Austria

[2]Center for Brain Research, Medical University of Vienna, Vienna, Austria

[3]Department of Clinical Neuroscience, Center for Molecular Medicine, Karolinska Institutet, Stockholm, Sweden

[4]Department of Neurotraumatology, Medical University Graz, Graz, Austria

[5]Center for Molecular Medicine, Department of Medical Biochemistry and Biophysics

Karolinska InstitutetStockholm, Sweden

Authors contribution:

S. Hochmeister was the initiator of both works and supported every publication and this thesis with indispensable knowledge. M. Ücal contributed equally to the second paper and was considered as co-first author. He was the major operator of all animal handling and

surgery of the cortical lesion model, assisted by K. Kraitsy, MT. Haindl and U. Schäfer. U. Köck led me through in situ hybridization and supported the result interpretation. L. Theisl was a lifesaver during histological staining procedure and animal handling assistance. J. Strasser was responsible for animal MRI during accomplishing paper 2, assisted by S. Ropele. F. Fazekas contributed to both works with valuable discussion and help in rephrasing the scientific texts. M. Zeitelhofer-Adzemovic characterized the lesions for paper 1 and provided the MOG for immunization procedures in the second paper with the help of M. Zeitelhofer. MT. Haindl was responsible for all histological preparations, stainings and microscopy pictures. I have also written the first paper and parts of the second paper and did all the quantification of the first paper. I was also responsible for statistical analysis in all papers under assistance of M. Ücal.

I have obtained permission to reproduce figures and tables from the respective copyright holders:

RE: reuse of own material for my dissertation

Permissions Helpdesk <permissionshelpdesk@elsevier.com>

Do 13.12.2018 19:07

An:Haindl, Michaela <michaela.haindl@medunigraz.at>;

Dear Michaela,

As an Elsevier journal author, you retain the right to Include the article in a thesis or dissertation (provided that this is not to be published commercially) whether in full or in part, subject to proper acknowledgment; see https://www.elsevier.com/about/our-business/policies/copyright/personal-use for more information. As this is a retained right, no written permission from Elsevier is necessary.

If I may be of further assistance, please let me know.

Best of luck with your dissertation and best regards,
Laura

Laura Stingelin
Permissions Helpdesk Associate
ELSEVIER | Global E-Operations Books
+1 215-239-3867 office
l.stingelin@elsevier.com
Contact the Permissions Helpdesk
+1 800-523-4069 x3808 | permissionshelpdesk@elsevier.com

ELSEVIER

Personal use

Authors can use their articles, in full or in part, for a wide range of scholarly, non-commercial purposes as outlined below:

- Use by an author in the author's classroom teaching (including distribution of copies, paper or electronic)
- Distribution of copies (including through e-mail) to known research colleagues for their personal use (but not for Commercial Use)
- Inclusion in a thesis or dissertation (provided that this is not to be published commercially)
- Use in a subsequent compilation of the author's works
- Extending the Article to book-length form
- Preparation of other derivative works (but not for Commercial Use)
- Otherwise using or re-using portions or excerpts in other works

These rights apply for all Elsevier authors who publish their article as either a subscription article or an open access article. In all cases we require that all Elsevier authors always include a full acknowledgement and, if appropriate, a link to the final published version hosted on Science Direct.

Copyright Clearance Center RightsLink®

Home | Create Account | Help

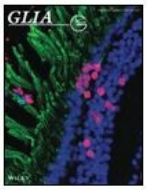

Title: The formation of a glial scar does not prohibit remyelination in an animal model of multiple sclerosis

Author: Michaela Tanja Haindl, Ulrike Köck, Milena Zeitelhofer-Adzemovic, et al

Publication: GLIA

Publisher: John Wiley and Sons

Date: Nov 28, 2018

Copyright © 2018, John Wiley and Sons

LOGIN

If you're a copyright.com user, you can login to RightsLink using your copyright.com credentials.

Already a RightsLink user or want to learn more?

Welcome to RightsLink

This article is available under the terms of the Creative Commons Attribution License (CC BY) (which may be updated from time to time) and permits use, distribution and reproduction in any medium, provided that the Contribution is properly cited.

For an understanding of what is meant by the terms of the Creative Commons License, please refer to Wiley's Open Access Terms and Conditions.

Permission is not required for this type of reuse.

Wiley offers a professional reprint service for high quality reproduction of articles from over 1400 scientific and medical journals. Wiley's reprint service offers:

- Peer reviewed research or reviews
- Tailored collections of articles
- A professional high quality finish
- Glossy journal style color covers
- Company or brand customisation
- Language translations
- Prompt turnaround times and delivery directly to your office, warehouse or congress.

Please contact our Reprints department for a quotation. Email corporatesaleseurope@wiley.com or corporatesalesusa@wiley.com or corporatesalesDE@wiley.com .

CLOSE WINDOW

Acknowledgements

The work of my thesis was carried out at the neuroimmunology lab of the Department of Neurology, Medical University Graz under the doctoral school of molecular medicine and inflammation. Primary financial support was provided by Medical University of Graz, Department of Neurology and Fresenius Kabi Austria in Graz (along with providing of vitamin D). All data about our new animal model was originally published in "Widespread cortical demyelination of both hemispheres can be induced by injection of pro-inflammatory cytokines via an implanted catheter in the cortex of MOG-immunized rats" by Ücal M, Haindl MT, Adzemovic MZ, Strasser J, Theisl L, Zeitelhofer M, Kraitsy K, Ropele S, Schäfer U, Fazekas F and Hochmeister S edited by Prof. Hoke and has been reproduced by permission of Elsevier. All material about astrocytic impact on remyelination was originally published in "The formation of a glial scar does not prohibit remyelination in an animal model of multiple sclerosis" by Haindl MT, Köck U, Adzemovic MZ, Fazekas F and Hochmeister S edited by Prof. Kettenmann and has been reproduced by permission of Wiley.

First of all I would like to thank my supervisor Assoz. Prof. Sonja Hochmeister for her support and presence. She wisely led me through all up and downs and was always there when I needed help. It is a rare luck to have such supervision. Second I would like to thank Priv. Doz. Willibald Wonisch for his support. Without his help and aid this thesis wouldn’t have been possible. His supervision was very professional, supporting and indispensable from the beginning on. He also managed the contact to Fresenius Kabi Austria, making our vitamin D experiments possible. Third I would like to thank Univ.-Prof. Franz Fazekas for the possibility to perform this thesis at the neuroimmunology lab and his support during all publications. He was always reachable when I needed his help and advice. I can proudly say that I had the greatest dissertation committee one can wish for.I want to thank Mag. Simon Brandstetter, product specialist of THP Medical Products, for his essential help in searching suitable antibodies for my huge staining requirements.I also would like to thank Johannes Strasser for his support and comprehension. I could always discuss every small or big problem during my thesis time and he could often solve those problems with his unique ideas.

Last but not least I want to thank my mom, Regina Haindl and my dad, Wolfgang Haindl – without you I couldn’t have come that far. I also want to thank my sister Angelika Haindl for her indispensable support during my bachelor studies – finally I managed to use units my dear sister.

Table of contents

Abbreviations and Definitions

A1	astrocytic phenotype associated with C3d thought to hinder remyelination
A2	astrocytic phenotype associated with S100A10, thought to enhance remyelination
A	active lesion
ABTS	2,2′-Azino-bis 3-ethylbenzthiazoline-6-sulfonic acid
BBB	blood-brain-barrier
C3d	complement system protein
C9neo	marker for complement deposits
Caspase3	a component of cytoskeleton, marker for apoptosis
CLM	cortical lesion model, an animal model for SPMS
CNS	central nervous system
DA	Dark Agouti – a rat strain
DAB	3,3'-diaminobenzidine, a substrate used for IHC
EAE	experimental autoimmune encephalomyelitis, an animal model for RRMS
ER	early remyelination
ELISA	Enzyme-Linked Immunosorbent Assay
GFAP	glial fibrillary acidic protein, a marker for astrocytes
IA	inactive lesion
IHC	immunohistochemistry, a technique to specifically target proteins in tissue
ISH	in situ hybridization, a technique to specifically target mRNA in tissue
IU	international unit
LFB	luxol fast blue, a myelin staining
LR	late remyelination
MOG	myelin oligodendrocyte glycoprotein (a myelin component)
mRNA	messenger ribonucleic acid
MS	Multiple Sclerosis
NAWM	normal appearing white matter
NeuN	surface protein of neurons, marker for neurons
NOGO	= RTN4 = reticulon 4, a marker for mature oligodendrocytes
NPCs	neural progenitor cells
OPC	oligodendrocyte precursor cell (indispensable for any remyelination process)
PBS	phosphate buffered saline
PFA	paraformaldehyde
PLP	proteolipid protein, a myelin component

PPm	polyphenol microtitre, a test for determination of protective polyphenoles
ROS	reactive oxygen species
RRMS	relapsing-remitting multiple sclerosis (usually first disease phase of MS)
RXR	retinoid X receptor
S100A10	S100 calcium binding protein A10
SP	shadow plaque
SPMS	secondary progressive multiple sclerosis (usually second disease phase of MS)
TAC	total antioxidative capacity
VDR	vitD receptor
vitD	vitamin D

Zusammenfassung

Unter dem Begriff Neuroprotektion versteht man den Schutz von Nervengewebe mit Hilfe von pharmakologischen oder molekularbiologischen Methoden mit dem primären Ziel den Krankheitsverlauf diverser Erkrankungen zu verbessern um in weiterer Folge die Lebensqualität der Patientinnen/Patienten zu steigern. Gerade wenn die ursächlichen zellulären Mechanismen von Erkrankungen noch nicht vollständig geklärt sind kommt der Neuroprotektion eine besonders hohe Bedeutung zu. Der Fokus dieser Dissertation liegt auf der neurologischen Erkrankung Multiple Sklerose (MS), deren Mechanismen zur Krankheitsentstehung noch nicht vollständig aufgeklärt sind. Bei MS handelt es sich um eine häufige Erkrankung des jungen Erwachsenenalters die zumeist mit einem schubhaften Verlauf startet und nach rund 25 Jahren in die sekundäre progrediente Phase übergeht mit stetiger Verschlechterung der neurologischen Symptome. Gerade hier sind Ansätze das Nervengewebe bestmöglich zu schützen und zu erhalten besonders wichtig.

Um diesem Ziel einen Schritt näher zu kommen ist Grundlagenforschung unabdingbar. Daher wurden in dieser Arbeit zwei Tiermodelle herangezogen, welche die humane zelluläre Situation sehr genau beschreiben können. Auf der einen Seite wurde eines der häufigsten MS-Tiermodelle verwendet, die experimentelle autoimmune Enzephalomyelitis (EAE), welche die zellulären Gegebenheiten der schubförmigen MS gut charakterisiert. Auf der anderen Seite wurde ein neues Tiermodell etabliert, das kortikale Läsionsmodell (CLM), welches viele der zellulären Besonderheiten der progredienten MS repräsentiert. Die Ergebnisse beider Projekte wurden dabei primär durch immunhistochemische Techniken erhalten, zusätzlich kamen kolorimetrische und enzymatische Testverfahren zum Einsatz.

Der Themenschwerpunkt an der Erforschung der EAE lag auf den Astrozyten, welche mannigfaltige Rollen bei immunologischen Geschehen, insbesondere bei MS, spielen. Vor allem (reaktive) Astrozyten, welche sich je nach Schweregrad des Schadens zu einer sogenannten Glianarbe ausbilden können, wurden lange kontrovers diskutiert. Diese Glianarbe wurde oft als eine undurchdringbare Barriere angesehen, die verhindert, dass Remyelinisierung stattfinden kann. Im Zuge dieser Dissertation konnte festgestellt werden, dass Reparaturprozesse - zumindest in diesem Tiermodell - trotz Ausbildung einer Glianarbe stattfinden können und sogar gefördert werden. Durch weitere Forschung könnten Astrozyten in Zukunft sogar ein Ansatzpunkt für neue remyelinisierungsfördernde Therapien werden.

Neue Therapieoptionen für MS Patientinnen/Patienten könnten sich auch über den zweiten Themenschwerpunkt dieser Dissertation ergeben. In unserem CLM konnten erstmals fast alle zellulären Besonderheiten der progredienten MS im Tiermodell dargestellt werden. Damit eröffnet dieses Modell die Möglichkeit potentielle neuroprotektive Substanzen zu testen um in Zukunft spezielle Therapien für MS Patientinnen/Patienten der progredienten Phase anbieten zu können. In einer ersten Austestung wurde Vitamin D (VitD) genauer betrachtet. Da dieses Vitamin in der schubförmigen MS und damit auch in der EAE als protektiv gilt, sollte herausgefunden werden, ob VitD auch potentiell in der progredienten MS-Phase hilfreich sein könnte. Dabei wurde entdeckt, dass Ratten, die ab der Entwöhnung von der Mutter mit VitD zugefüttert wurden wesentlich weniger zelluläre Schäden aufwiesen als jene Tiere, die kein VitD zugefüttert bekamen. Diese Daten könnten ein Hinweis darauf sein, dass VitD in Zukunft - nach näherer Erforschung - auch eine sinnvolle Ergänzung in der Therapie der progredienten MS sein könnte.

Zusammenfassend konnten in dieser Dissertation zwei Hauptprojekte bearbeitet werden, wobei in beiden Modellen wichtige neue Erkenntnisse auf dem langen Weg zur Neuroprotektion erforscht werden konnten.

Abstract

Neuroprotection describes the prevention of damage to nerve tissue via pharmacological or molecular biological methods with the aim to influence the course of the disease and improve the quality of life for patients. In order to reach this aim it is necessary to investigate the cellular background of the respective diseases to allow to intervene at distinct cellular pathways.

This thesis focused on the mechanisms of tissue damage and repair in Multiple Sclerosis (MS). MS is an inflammatory demyelinating disease of the central nervous system mainly affecting young adults. Most patients start with a relapsing-remitting (RR) disease phase and enter a secondary progressive (SP) phase after a duration of approximately 25 years. Histologically, these disease stages are very different. To investigate cellular characteristics of RRMS and SPMS two different animal models were used, hence this thesis comprises two separate projects. The methods used included immunohistochemistry, colorimetric testing, enzyme-linked immunosorbent assays and in-situ hybridization.

In the first project, a common animal model for MS, the experimental autoimmune encephalomyelitis (EAE), which resembles the cellular characteristics of human RRMS quite well, was used. The investigation focused on (reactive) astrocytes and the biological characteristics of the glial scar and its influence on repair processes after inflammatory demyelination. Most often the glial scar is thought of an impenetrable barrier to remyelinating oligodendrocytes, hindering any repair. In our study however we were able to show that at least in this animal model of EAE the formation of a glial scar does not prohibit remyelination but actually can even facilitate repair.

In the second project a new animal model, the cortical lesions model (CLM), which resembles most of the cellular characteristics of human SPMS brain pathology, was established. Apart from establishing the model, CLM was used to investigate the role of oxidative stress and the effect of vitamin D (vitD) supplementation on cortical pathology. It is demonstrated that in this CLM model vitD has a protective effect and ameliorates the disease course at least when the animals receive a preventive vitD supplementation right after weaning from their mothers.

This thesis resulted in two main novel findings. It allows a new view of the glial scar and might lead to new neuroprotective strategies by enhancing astrocytic factors in different stages of repair. Secondly, this thesis introduces a new animal model reassembling many features of cortical pathology of human SPMS and offers the opportunity to test potentially

neuroprotective and repair- facilitating agents directly in the brain lesions. Additionally the promising findings on vitD suggest further research to identify ways to therapeutically use vitD supplementation for SPMS patients.

Introduction

Symptoms of brain diseases vary widely. Acute brain injury, caused by inflammation or any other insult is associated with short and long-term morbidity and mortality. Following the primary cerebral damage a cascade of events amplifies the initial damage. Secondary biochemical changes contribute to subsequent tissue damage and are associated with neuronal cell death, but at the same time beneficial cellular effects can also occur. The time course over which these effects appear may be longer than assumed previously.

In this thesis we want to focus on the mechanisms of tissue damage and repair in immune mediated conditions of the central nervous system. For our investigation we use different models of Multiple sclerosis (MS). MS is an inflammatory demyelinating disease of the central nervous system (CNS) mainly affecting young female adults (mean age of onset 27 years). The target of the immune reaction is the myelin sheath, the cover around axons. The disease is characterized by a heterogeneity of clinical symptoms, a variable radiological appearance and histological differences of lesions in different stages of de- and remyelination affecting the response to therapy (1). Most patients start with a relapsing-remitting (RR) disease phase characterized by alternating demyelination followed by subsequent recovery. After a duration of approximately 25 years many patients enter a secondary progressive (SP) disease phase characterized by a progredient worsening of clinical neurological symptoms without much accompanying inflammation (2). Consequently the pathogenesis of MS is controversial and there is no effective universal treatment that fits all (1,3). Because of its heterogeneity of both the RRMS and the SPMS the largest research field of MS is still focused on improving therapeutics for RRMS and find new specific treatment for SPMS. One main focus is to investigate the underlying mechanisms further to understand cellular interplay leading to possible new therapeutic options.

Cellular characteristics of MS

T- and B-cells play a key role in the pathogenesis of MS. Those cells might be selectively recruited by specific CNS target antigens resulting in inflammation affecting only the CNS (4,5). The innate immune system also has an important role in the initiation of the disease. Macrophages promote the pro-inflammatory response of T- and B-cells and early microglial activation might be an initial event in lesion development. Activated microglia could contribute to disease pathology through several pathways including secretion of pro-inflammatory cytokines, chemokines, free radicals and release of glutamate. Cellular characteristics in early stages of MS are thus focal white matter injuries associated with

macrophages and lymphocytic infiltrates predominantly seen near blood vessel (inflammatory cuffs). The relapses in RRMS depend on both the location of the CNS region affected by the demyelination and the extent of the inflammatory process (4).

The contribution of the peripheral immune system decreases during progressive disease phase and the immune response is suggested to be confined to the CNS. Due to the longer disease course inactive lesions and slowly expanding demyelination have a higher prevalence in SPMS compared to RRMS (6). CNS pathology changes to diffuse white matter injury associated with microglial activation and diffuse lymphocytic infiltrates. This is accompanied by increasing cortical involvement which is thought to be associated with lymphoid-like follicles in the meninges (7). In SPMS tissue injury is also caused by degeneration of chronically demyelinated axons, and damage or dysfunction of astrocytes. Loss of myelin trophic support, leading to progressive swelling and cytoskeletal disorganisation of chronically demyelinated axons could be unique to the SPMS (4).

It is important to keep in mind that MS is a very heterogeneous disease and those characteristics described above are fitting to the majority but not all patients. Extensive oligodendrocyte apoptosis, microglial activation and few or no lymphocytes or myelin phagocytes could be found in the absence of blood-brain-barrier (BBB) derangement, demyelination and axonal loss in some RRMS as well as in SPMS patients. Thus other mechanisms of MS lesion formation initiation has been suggested, in agreement with the identification of extracellular myelin in leptomeninges and perivascular spaces. A primary myelin trafficking from the CNS to the secondary lymphoid organs is suggested for further antigen presentation to sustain the autoimmune neuroinflammatory response (6,8).

The hallmarks of MS pathology are axonal damage or neuronal loss, demyelination and astrogliosis. Axonal or neuronal cell loss is referred to as neurodegeneration and is in particular relevant because it is the main reason of permanent clinical disability. Whole brain atrophy in MS occurs at rates of 0.5 - 1.5 % per year and even increases during SPMS (9). Patients with newly diagnosed MS have already axonal loss and other damage. Therefore an early treatment and suitable strategies to promote remyelination and prevent further damage is very important (1).

The role of oxidative stress in neurodegenerative diseases

A crucial role in onset and progression of neurodegenerative diseases is related to oxidative stress (10,11). Oxidative stress leads to dysregulation of the inflammatory response and a disturbance of the antioxidant defense system is often a key point to

disease mechanisms. The main characteristics of the oxidative stress state are an increase of reactive species levels and a weaker antioxidant system, failing to ward free radicals (11). Especially the inability of the antioxidant defense system to modulate an accurate response is a key to the onset and progression of those diseases. Due to the loss of redox homeostasis intracellular signaling pathways are altered leading to a change in signal transduction. This leads in addition to the secretion of pro-inflammatory molecules, to a promotion of neuroinflammation in the CNS. While in a healthy, balanced system, the inflammatory response is a finely regulated defense mechanism, the chronic loss of redox balance in neurodegenerative diseases the immune response is dysregulated and pro-inflammatory responses dominate. Reactive oxygen species (ROS) furthermore stimulate activation of astrocytes, microglia and $CD4^+$-T-cells (11). In MS the lesion formation and recruitment of monocytes, which are the major producers of ROS are related to oxidative stress, propagating autoimmune-mediated tissue damage. This effect has not only been observed in MS but also in related animal models (10,11). Studies of MS autopsy material point towards demyelination as a cause of oxidized lipids present in myelin membranes, apoptotic oligodendrocytes and axons (11).

Treatment with antioxidants might prevent tissue damage and improve survival on a cellular level and in turn improve neurological outcome of the disease. One parameter that is modulated either by radical overload or by intake of antioxidants is the total antioxidant capacity (TAC) of plasma (10). Dietary intake of polyphenols is known to attenuate oxidative stress and reduce the risk for MS and other neurodegenerative diseases. Preclinical studies have shown that polyphenols exhibit potential to block neural inflammation and damage along with modulation of inflammatory cytokines. This potential of polyphenols makes them a desirable research aim as a therapeutic in MS (12).

Impact of Vitamin D (vitD) on MS

One particular antioxidant thought to enhance the defense system in several neurodegenerative diseases is vitD. VitD is amongst others essential for lymphocyte activation, T-cell differentiation, the production of specific antibody isotypes and the regulation of the immune response (13). Many studies have suggested that there is a correlation between the level of serum vitD and MS disease activity and onset. A positive effect of vitD could be observed in well established animal models for RRMS (14). Some studies show also an association of MS with low levels of vitD and a benefit derived from its supplementation (13,15). It remains unclear if a positive effect can be achieved in SPMS as well and if these patient group could benefit from a supplementation due to lack of knowledge of pathophysiological mechanisms of SPMS. However, a positive result

could come along with a huge benefit for patients due to the easy handling of vitD supplementation.

Endogenous repair in MS

MS lesions, especially in the early phases of the disease course, may be at least partially repaired by remyelination which means that specialized cells, oligodendrocyte precursor cells (OPC) migrate into the lesion area, further differentiate to myelinating oligodendrocytes and replace the missing myelin sheath. However sometimes remyelination fails completely, depending on various conditions including presence of extrinsic inhibitors in lesions, insufficient pro-regenerative factors and impaired intrinsic capacity in OPCs. Remyelination failure can be segregated into two distinct phases – impaired recruitment of OPCs into the lesion and failure of differentiation or maturation of OPCs. It is important to realize that interrupting one stage can affect the other and that some factors can act at multiple stages. Thus understanding myelin and axonal repair strategies is a very important research aim (16,17).

Repair mechanisms in RRMS

Reappearance of oligodendrocytes within active lesions associated with early stages of remyelination are seen in patients with RRMS. This remyelination has been suggested to be transient and may be affected by new demyelination. White matter lesions are thought to be a direct consequence of inflammatory cellular infiltrates consisting mainly of lymphocytes and macrophages located around veins (18). Histopathological RRMS patients exhibit inflammatory damage bordered by a glial scar. The glial scar is associated with a rearrangement of tissue structure and astrocyte proliferation. Mild to moderate astrogliosis is believed to protect from oxidative stress, facilitates the blood-brain barrier repair and limits the spread of inflammatory cells from damaged areas into healthy CNS tissue (17,19–21). On the other hand the glial scar is often described as rigid border impenetrably for remyelinating cells even suggesting astrocytes deletion as therapeutic target (22).

Repair mechanisms in SPMS

In patients with SPMS remyelination is most often sparse and largely restricted to the borders of inactive plaques. Yet partial and full remyelinated areas can be found in those patients as well (23). Cortical pathology is a common finding of SPMS patients. Histologically these cortical lesions differ to the white matter lesions by a relative lack of cellular infiltrates, extensive microglia activation and apoptotic neurons (18,24,25). It is still unclear if cortical and white matter lesions are caused by different disease mechanisms or

if it is the same underlying mechanism but amended by influences of the local microenvironment.

Current therapies for multiple sclerosis include immunosuppressive or immunomodulating drugs, but these are aiming at suppressing inflammation and are not effective in the progressive phase, as the exact mechanisms of tissue damage and repair in this disease are at present not fully understood. Especially the interplay between different cell types in creating a microenvironment favoring or discouraging repair processes is only partly understood and can vary depending on multiple factors (17,18). The limited success of anti-inflammatory drugs in the treatment of SPMS suggests that other neuroprotective or repair-promoting strategies should be developed. Cellular energy metabolism seems to be abnormal in SPMS too and hence is another potential therapeutic target such as the involvement of vitamins. Also cell-based repair-promoting strategies could be very promising for example aiding OPCs (26).

Development of myelin repair strategies

For testing repair efficiency of potential candidates animal models are indispensable. The most commonly used animal model is the experimental autoimmune encephalomyelitis (EAE) in rodents. It models autoimmune inflammation quite well. Because of its similarity to inflammatory injury in MS it has been important in the validation of current MS therapies (16). One limitation is the difficulty in predicting size and localization of the demyelinating lesions. A common alternative to EAE are the toxic induced demyelination models. One common used model is the cuprizone model, where animals are fed with cuprizone, a copper chelator. In this model the demyelination is limited to the corpus callosum and superior cerebellar peduncle. The ongoing axonal injury in this model makes it an important implement to study the inter-relationship between remyelination and axonal survival. To better define the location and size of lesions in some models local injections of myelinotoxic agents are used (27). Those injections kill oligodendrocytes and astrocytes and lead to demyelination. The benefit of this model is that there is an acute injury in a localized area and a subsequent inflammatory response allows investigation of remyelination in the absence of ongoing damage. A disadvantage is that the inflammatory response occurs without the chronic involvement of lymphocytes that is typical for MS (16). All those models are very useful and important to monitor cellular characteristics of MS but are not able to exhibit the total complex environment of MS lesions in patients which contain numerous remyelination inhibitors and are exposed to several therapeutic approaches over very long periods of time (16).

Strategies to improve repair

Repair mechanisms are strongly dependent on the respective microenvironment. It is thus very important to search new cellular mechanisms and connections to find more possible ways to improve repair mechanisms.

Ideally, medications for MS should promote the repopulation of OPCs, accelerate differentiation and maturation of OPCs or overcome impediments in the lesion microenvironment (16). These compunds could be used along with immunomodulatory agents. Because remyelination is one part of neuroprotection, medications for myelin repair could provide benefit throughout the entire disease course. Many challenges remain including balancing repair versus injury, ensuring that medications can enter the BBB, defining the objective means to monitor remyelination and determining which medications are the best options with reasonable clinical outcomes (16). In the following, potential repair enhancing strategies are summarized.

Targeting neuronal activity

By silencing electrical activity myelination is reduced without affecting oligodendrocyte numbers and vice versa, indicating a key role of electrical activity in the myelination process (27). These results were further confirmed with the identification of adenosine and glutamate released from astrocytes and along axons as molecular mediators of activity dependent myelination. These findings extend recent research that social experiences and altered neuronal activity can influence myelin plasticity and are able to influence a functional outcome. New therapeutic development could target neuronal activity to promote disability improvement (27).

Cells achieving remyelination by promoting OPCs

Remyelination in the CNS is achieved by parenchymal oligodendrocyte precursor cells (OPCs), which persist in the adult CNS (approximately 5% of total cells in the brain). Those OPCs are able to generate new oligodendrocytes that contribute to remyelination following demyelinating events. The transcriptomic profile of adult OPCs is more similar to that of adult mature oligodendrocytes than from neonatal OPCs. Interestingly, these OPCs are not the only remyelinating cells of the adult brain. Oligodendrocytes might be generated from subventricular neural progenitor cells (NPCs) as well. NPC-derived oligodendrocytes are the major contributors of remyelination in the corpus callosum and myelin sheaths generated by those cells are thicker than those produced by OPCs. Mature Oligodendrocytes however do normally not contribute to remyelination and are therefore no target for regenerative therapy (27). One possible repair enhancing strategy

is therefore the promotion of proliferation and/or recruitment of OPCs by the addition of mitogens. In culture oligodendrocyte proliferation facilitates myelination and differentiation but proliferation of OPCs alone did not lead to appropriate remyelination in animal models. Therefore promoting oligodendrocyte differentiation is the preferred accompanied strategy to enhance remyelination in MS (16). One requirement for oligodendrocyte-differentiation-promoting medication is that they have to cross the blood-brain-barrier. But even if they do and if they improve remyelination in animal models in which spontaneous remyelination is robust, they may not promote remyelination in MS patients. Inhibitory molecules are responsible for slowed remyelination in the aged brain and during remyelination in the MS brain, which may counteract the benefits of such medications. Some medications promote remyelination in a robust regenerating system but they may be less effective in an inhibitory microenvironment (16).

Anti-inflammatory, immunomodulatory agents

Anti-inflammatory agents are of particular interest in early phases of MS. They control the detrimental aspects of inflammation and neuronal injury caused by immune cells that might be reduced (16).

Overcoming inhibitors within lesions

Numerous molecules have been identified to prohibit OPC differentiation and thus act as potential remyelination inhibitors. It seems that the extracellular matrix in MS lesions is a complex network of interacting proteins affecting remyelination. A predominant anchor that is crucial to regulate remyelination remains to be established. The activity of retinoid X receptor-α (RXRα) is important in oligodendrocyte linage cells. The expression of RXRγ is suggested to correlate with remyelination capacity in MS lesions. Apart from that, RXRγ binds to other nuclear receptors including vitD receptor (VDR). These RXR-VDR complexes promote oligodendrocyte differentiation. RXR and VDR agonists improve white matter regeneration through multiple cell types and are thus of therapeutic interest (16).

Aim of this thesis

Neuroprotection is defined as an intervention that influences the disease process or pathogenesis – favorably leading to lasting benefits for patients (28). Accordingly, in this thesis we focus on repair mechanisms and how to improve them. For this purpose we investigated repair mechanisms in diverse animal models of MS. In order to cover the different aspects of human MS we focused on two different models – on the one hand a common experimental autoimmune encephalomyelitis (EAE) model with a close cellular similarity to human RRMS and on the other hand our recently established cortical lesions

model (CLM, (18)) resembling most of the cellular properties of the SPMS. Results might give rise to new ideas on neuroprotective therapeutic strategies. Figure 1 gives an overview of the connections between the different topics within this thesis.

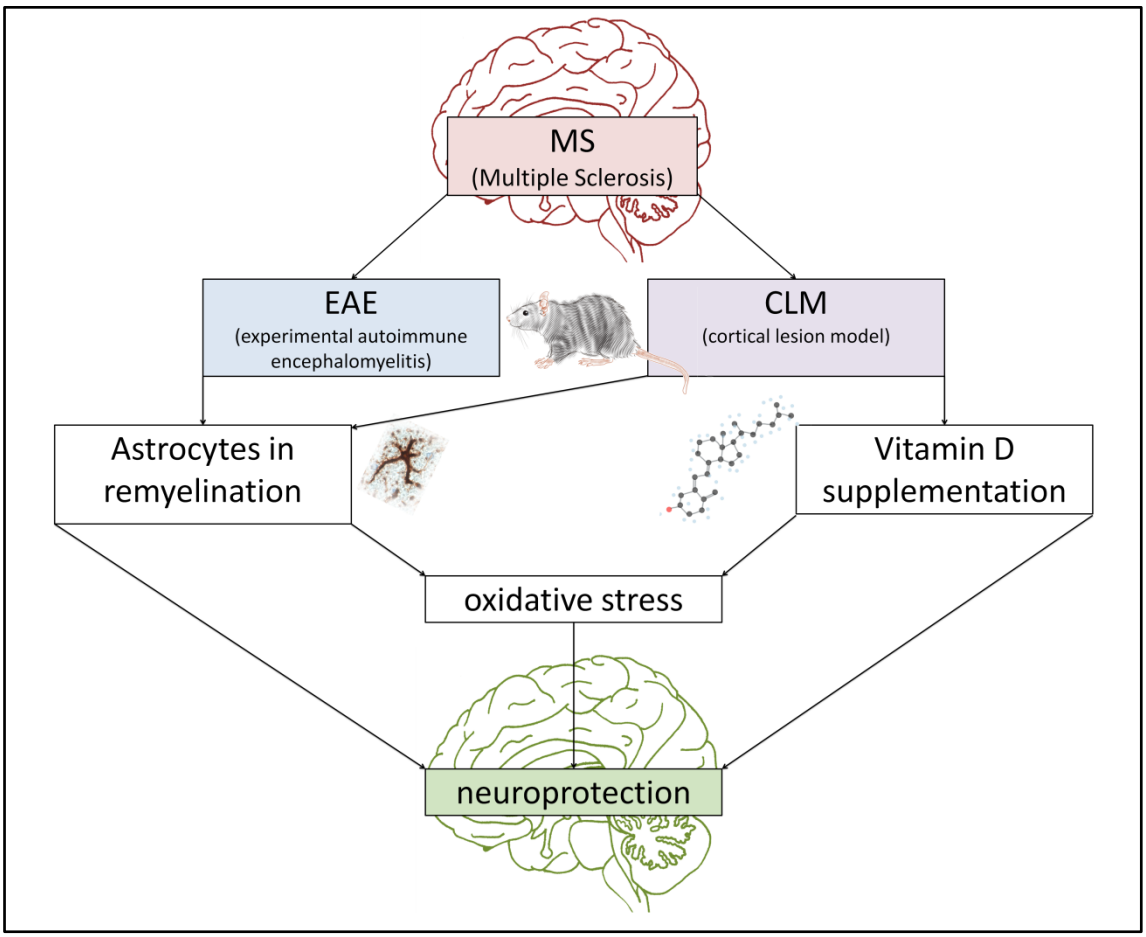

Figure 1: Dissertation Scheme. Overview of the connections between the different topics within this thesis. Based on MS research we used two different animal models, the EAE and our new CLM. With respect to the EAE model our research was focused on astrocytes and their involvement during lesion development and repair. The new CLM is introduced in this thesis and first results of vitD supplemented animals are represented in comparison to normal, untreated experimental conditions. Astrocytes seem to play an important role in our CLM too since oxidative stress affects pathomechanisms in both EAE and CLM.

Thesis development

First we focused on repair mechanisms of EAE. We knew that the negative view of the glial scar still persists and even found literature suggesting to eradicate astrocytes as a new therapeutic strategy. This seemed to us a harsh idea since the complex role of astrocytes is only partly investigated yet. In order to contribute to astroglial research we started to trace astrogliosis and repair mechanisms in the very well characterized EAE model with the opportunity to look closely at all white matter lesion stages from active demyelination to fully accomplished repair. As we found first evidence that the glial scar

does not prohibit remyelination, we further traced factors produced by astrocytes known for their influence on remyelination (described in literature both detrimental and facilitating). Our data points to a very complex interaction between astrocytes and their environment as well as the different astrocytic phenotypes. At the same time we were establishing our new CLM with the idea to provide a model with close similarity to human SPMS brain pathology. A feature of our CLM is the possibility to test different remyelination supporting substances either directly through the catheter or via systematically supplementation. The positive effect of vitD was already investigated in EAE (14) but not yet in CLM. This led us to the idea of investigating remyelination properties of our CLM with animals supplemented with vitD. Since vitD is a potent antioxidant we furthermore wanted to use some biomarkers for oxidative stress to support our histological findings. This lead us to the dual research during this thesis.

Material and Methods

Experimental autoimmune Encephalomyelitis (EAE)

We choose EAE for studying the full course of lesion evolution from active demyelination up to successful remyelination and furthermore, to evaluate the correlation between the extent of astrogliosis and remyelination. This study was performed on archival material of female DA/OlaHsd rats 8-10 weeks actively immunized with recombinant rat myelin oligodendrocyte glycoprotein (MOG) collected within the archives of the neuroimmunology research laboratory between 1998 until present (17,29–31). For our investigation we selected material form animals with clinical symptoms and large confluent lesions, which led to a total of 45 rats. Lesions were classified as active lesions (A), inactive to early remyelinating lesions (IA/ER), early to late remyelinating lesions (ER/LR), late remyelinating lesion to shadow plaque (LR/SP) and successful remyelination, the shadow plaque (SP) (17).

Immunohistochemistry (IHC)

For all IHC stainings, serial paraffin sections from 1.5 to 2 µm were prepared. Slides were stained for luxol fast blue (LFB) to obtain a first overview on tissue inflammation and demyelination (17).

First of all, slides were dewaxed in Xylene (Roth, Karlsruhe, Germany), rehydrated and incubated in a methanol solution containing H_2O_2 (Merck, Darmstadt, Germany). Antigen retrieval was performed using EDTA (Sigma, Sankt Louis, MO, USA) at pH 5.2 in a steamer for 1 hour. After a cooling step, slides were washed and blocked for 20 minutes with 10% fetal calf serum (FCS; Sigma) in DAKO REAL antibody diluent (Dako; Santa Clara, CA, USA). The blocking solution was discarded and the primary antibody was applied diluted according to the information given in supplementary table 1 in FCS/DAKO and incubated over night at 4 °C. After three washing steps with phosphate buffered saline (PBS) the secondary biotinylated antibody (GE Healthcare, Buckinghamshire, Great Britain) was applied 1:200 diluted in FCS/DAKO and incubated at room temperature for 60 minutes. Coated with peroxidase labelled avidin (Sigma) diluted 1:100 in FCS/DAKO slides were incubated at room temperature for 60 minutes. Visualization of the primary antibody was performed with 3,3’-diaminobenzidine (DAB; Sigma) and counterstaining with hematoxylin (Gatt-Koller, Absam, Austria). Slides were dehydrated in ascending ethanol concentrations and covered with Shandon Consul-Mount (Thermo Scientific, Waltham, MA, USA) and a cover slip (17).

For all IHC double stainings pretreatment procedures were performed as described above. Two desired antibody solutions respectively were incubated simultaneously in FCS/DAKO at 4 °C overnight on selected lesions. For detection of primary antibodies, a polymer-based detection system (ImmPRESS; Vector Laboratories, Burlingame, CA, USA) was used according to the manufacturer's instructions. Visualization of anti-mouse ImmPress reagent was performed with DAB (Sigma) and visualization of anti-rabbit ImmPress or anti-goat ImmPress reagent respectively was obtained with VIP Peroxidase substrate kit (Vector Laboratories). Slides were afterwards dehydrated and covered with Shandon Consul-Mount (Thermo Scientific) and a coverslip. Further information about all used antibodies can be found in supplementary table 1 (17).

In-situ-Hybridisation (ISH)

For all ISH stainings serial paraffin sections from 1.5 to 2 µm were prepared under RNase-free conditions. All steps were conducted with diethylpyrocarbonate enriched (DEPC; Sigma) water. The paraffin embedded tissue sections were dewaxed in Xylene (Roth) and rehydrated. To fix the intersections, slides were incubated in 4 % PFA (Merck) for 20 minutes. After washing steps in tris-buffered-saline (TBS; Merck) slides were incubated in 0.2 M HCl (Sigma) for 10 minutes. Pretreatment was performed with 20 µg/mL proteinase K solution (Sigma) for 20 minutes at 37° C. After stopping the enzyme activity in TBS at 4° C, slides were incubated in 0.5 % acetic anhydride (Sigma) under stirring for 10 minutes to block the endogenous alkaline phosphatase reaction. Slides were dehydrated and incubated in a wet chamber at 55 °C for 30 minutes. The full length probes (kindly provided by the institute of brain research Vienna), were applied, coverslipped and incubated for exactly 4 minutes on a 95 °C heating plate. Hybridization occurred over night at 65 °C. On the following day slides were washed and incubated in Boehringer blocking reagent (Roche, New Jersey, IN, USA) with 10% FCS for 15 minutes. Anti-digoxigenin antibodies conjugated with alkaline phosphatase (Roche) were applied 1:500 in blocking reagent with 10% FCS for 1 hour. The sections were developed with NBT/BCIP (Roche) at 4 °C under microscopic controls (17).

For the IHC double staining, mouse proteolipid protein (PLP) primary antibodies were applied diluted 1:1000 in 10% FCS/TBS over night at 4 °C. After three washing steps, the biotinylated secondary mouse antibody (GE Healthcare, Buckinghamshire, Great Britain) was applied 1:200 in FCS/TBS 1 hour at room temperature. Subsequently, incubation with avidin-alkaline phosphatase complex (Roche) was performed for 1 hour at room temperature. The slides were developed using a fast red solution (Sigma). Counterstaining was performed with hematoxylin and slides were coverslipped (17).

Histopathology and quantitative evaluation of EAE

White matter lesions in MOG EAE are more often located in the spinal cord. Lesions were identified and analyzed with respect to lesion types as described above. Adjacent slides of each lesion were subjected to IHC for GFAP to detect the astrocytic reaction and ISH for PLP mRNA to monitor remyelinating OPCs in spinal cords. Analysis was performed by a single blinded investigator (Michaela Tanja Haindl) for lesion types. The selected lesions were quantitatively assessed on a Zeiss Axioplan2 imaging light microscope with a counting ocular. All specifically stained cells for the respective antigen were quantitatively assessed in one full square grid and results converted into corresponding cells per mm^2. We chose GFAP as marker for astrocytes because it is an intermediate filament which means that the whole cell body is stained quite well and makes it a practicable marker for quantification (17).

Quantitative evaluation of double labeled cells

For IHC double staining experiments we selected 20 representative lesions (selected out of 15 rats) from every lesion type and normal appearing white matter (NAWM) according to best GFAP staining results and tissue quality of the whole sample set. As there are many factors expressed by astrocytes known to intervene during remyelination we selected only a small subset composed of semaphorins 3A and 3F (Sema3A, Sema3F), hyaluronan (detected via hyaluronan binding protein 2, HABP2), bone morphogenetic protein-2 (BMP-2), ciliary neurotrophic factor (CNTF), brain-derived neurotrophic factor (BDNF), CXC-motif-chemokine 12 (CXCL-12), fibronectin 1 (FN1), tenascin C (Tn-C) and insulin-like growth factor (IGF) (17).

Double labeled cells of GFAP and the respective astrocyte derived factor were counted within the lesions by using an ocular morphometric grid. The size of the grid with appropriate magnification was 313 µm × 313 µm. The values were then transformed to cells per mm^2. The quantification of all factors in each lesion type is given as percentage scale. All detected GFAP positive astrocytes represent 100% and the corresponding ratio illustrates the detected double labeled cells in the same area (17).

Evaluation of astrocytic phenotypes A1 and A2 in EAE

In order to follow the two different astrocytic phenotypes A1 and A2 over the full course of lesion evolution we chose the markers described by Liddelow et. al. 2017; C3d complement for detecting A1 and S100 calcium-binding protein A10 (S100A10) for A2 (32). We documented the results via selected microscopy pictures (17).

Statistical analysis

All statistical calculations and graphic illustrations were performed using IBM SPSS Statistics 23 and graphs were illustrated in Microsoft Excel 2010. All box and whiskers plots in this thesis show the median as a line and the upper and lower quartiles as boxes. The ends of the whiskers are 1.5 times the interquartile range above and under the third and first quartile. Stars above and under the whiskers represent the minimum and maximum outliers. All data sets of continous variables were checked for normal distribution (Kolmogorov-Smirnov test) with most of the variables being not normally distributed. Because of this and the ordinal lesion evolution we used the non-parametric Kruskal-Wallis test ($p < 0.05$) to assess statistical differences between groups. With this test we could detect significant differences and therefore added an analysis using the exact Mann-Whitney U test for multiple comparison with Bonferroni correction (a cutoff for the p-value of 0.01 was considered significant) (17).

Cortical lesion model (CLM)

We chose our CLM (18) for evaluating repair enhancing properties of Vitamin D and for studying cellular features of cortical lesions. In short the experimental setup is displayed in figure 2.

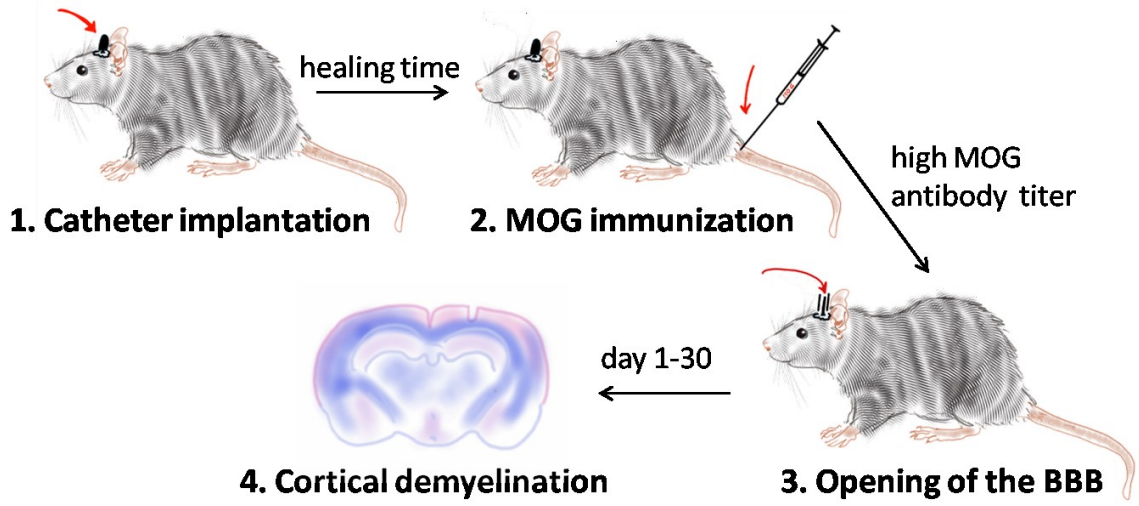

Figure 2: Scheme of our CLM. The experiment starts with a catheter implantation. After a healing time rats are immunized with MOG. The BBB is opened via injection of pro-inflammatory cytokines through the catheter directly into the brain. Cortical pathology can be investigated from day 1-30 with the possibility of another "relapse" via second cytokine injection on day 30. Drawings and word art by Michaela Tanja Haindl.

The experiment starts with the catheter implantation directly into the frontal lobe of the brain. After a healing period of two weeks animals get immunized with MOG. Once the animals develop a sufficient anti MOG antibody titer the BBB is opened via injection of

pro-inflammatory cytokines (Interferon gamma and tumor necrosis factor alpha) through the catheter. This leads to cortical demyelination starting from day 1 after cytokine injection with close similarity to human SPMS brain (18).

A total of 65 male Dark Agouti (DA) rats age 10-12 weeks, obtained from Harlan, Netherlands or Janvier, France were used for establishing the model. For investigation of the vitD impact on cortical pathology additionally 24 animals were subjected to the same experimental setup as described above but with supplementation of vitD during the whole experiment, starting right from weaning of the pubs from their mothers (1 drop Oleovit, Fresenius, Austria = 400 IU per week). The total number of different animal groups used in this thesis is listed in supplementary table 2. Before any surgery was performed animals were kept in groups of four. After catheter implantation the animals were moved to modified single cages (cages with a acrylic glass protection on lowered railing) to avoid damage to the catheter. All animals were housed in a 12 h light/dark cycle with food and water provided *ad libitum*. All animal experiments were carried out under approval of the local authorities (Bundesministerium für Wissenschaft und Forschung; BMWFW-66.010/0132-WF/V/3b/2014 & BMWFW-66.010/0072-WF/V/3b/2017) (18).

Blood samples and Enzyme-linked immunosorbent assay (ELISA) for CLM

Blood samples were obtained four weeks after immunization and serum IgG antibody titeres against MOG were determined by ELISA. In short, MOG (5 µL MOG/ml PBS) was coated on a 96 well plate (Nunc, Wiesbaden, Germany) and incubated for 1 hour at 37 °C. Then the plate was blocked with 1 % bovine serum albumin (Sigma) in PBS for 1 hour at room temperature. Afterwards the plate was incubated with rat sera (1:50) and standard for 2 hours at 37 °C. IgG specific anti-rat antibody (1:10 000) was used as conjugate. 2,2′-Azino-bis 3-ethylbenzthiazoline-6-sulfonic acid (ABTS) was added as substrate. Between these steps the plate was washed three times with PBS/Tween (Merck). The optical density was measured at 405 nm (18).

Euthanasia and Tissue Extraction CLM

Groups of animals were euthanized on day 1, 3, 15 and 30 after cytokine injection and on day 15 after a second demyelination phase under deep anesthesia with Midazolam, Fentanyl and Medetomidin, followed by cardial injection of 25 mg Thiopental (Sandoz, Kundl, Austria; 0.5 ml, 50 mg/ml concentration) and transcardial perfusion of 4% paraformaldehyde (PFA; Merck, Darmstadt, Germany) in PBS. Brains and spinal cords were dissected, post-fixed in 4% PFA for 24 hours and routinely embedded in paraffin (18).

IHC staining

IHC staining was applied exactly in the same way as described under the EAE Methods section.

Histopathology and quantitative evaluation of CLM

For quantification of demyelination and cellular components adjacent serial sections of the catheter insertion area were used. Demyelination was quantitatively assessed by quantification of cortical loss of PLP immunoreactivity using an optical grid; the loss of PLP immunoreactivity in each group was quantified for each hemisphere and values were then transformed to mm^2 (18).

Apoptotic cells (Caspase3), neurons (neuronal nuclei marker; NeuN) and activated microglia (ionized calcium-binding adapter molecule; Iba1) were assessed in three full optical grids in the cortex per hemisphere; average values were then converted to cells/mm^2. Quantification was performed by a single blinded investigator for each representative slide per staining. We also systematically assessed the spinal cords of all experimental animals in histology for inflammation or demyelination to exclude extracerebral pathology (18).

Statistical analysis

All graphs were illustrated as described under the EAE statistical analysis section. We used various control groups (18) which were pooled as a single control group unless a statistically significant difference was observed (tested with Mann-Whitney U Test, cut off for p-value: 0.01). Statistical significance of the changes observed in experimental groups in comparison with the control group and the vitD groups was assessed with Mann-Whitney U Test. A difference with $p < 0.05$ was considered to be statistically significant in a single test (18).

Colorimetric/photometric test systems for oxidative stress

Total anti-oxidative capacity (TAC)

The TAC test is a colorimetric test to measure antioxidants in sera. It is based on the reaction between hydrogen peroxide, horseradish peroxidase and tetramethylbenzidine to give a blue-green color. After the addition of the stop solution the color changes to yellow and can be measured at 450 nm. A linear standard curve was used for quantification (33,34). The whole test was kindly adapted for small sample volumes by Prof. Willibald Wonisch. Blood samplings of our vitD supplemented animals and controls were performed

on day 1 – 30 after cytokine injection and on day 15 after second cytokine injection. Serum was obtained by centrifugation at 4600 rpm one hour after blood sampling and was stored at -70 °C until use. All samples were analyzed in double. The assay was performed according to the manufacturer´s instructions with distinct modifications for the measurement of small sample volumes. Reagent A consisted of 4 mL assay buffer and 4 µL peroxide. Reagent B consisted of 2.5 mL assay buffer, 25 µL substrate and 2.5 µL peroxidase. In a 96 well microtiter plate 10 µL standard controls and samples (undiluted) were pipetted. 40 µL of reagent A were pipetted into all wells within 1 minute. Subsequently, 20 µL of reagent B were pipetted into all wells – within another minute. The test was incubated for exactly 20 minutes at 4 °C. The experiment was stopped by the addition of 20 µL stop solution. The absorbance was measured at 450nm by using a microplate reader.

Polyphenols-microtitre (PPm)

PPm test measures total polyphenols in fluids. The detection is based on the reaction of polyphenoles with transition metals. This leads to a brown/black-colored complex, which can be measured at 766 nm. A linear standard curve was used for quantification (33). Serum of vitD supplemented animals and controls were collected as described above. All samples were analyzed in repeated in double. In each well of a microtiterplate we used 20 µL of prediluted samples (5 µL of rat serum in 45 µL diluent). Furthermore, 50 µL of diluent, 100 µL of reagent and 30 µL of intensifier was pipetted in each well according to the manufacturer's instruction. The reaction components were mixed thoroughly by putting the plate on a horizontal shaker. After an incubation time of 2 hours the optical density was measured on a plate reader at 766 nm.

Results

EAE results

Histopathological results in rat spinal cord

Figure 3 illustrates in detail the characteristics of the different lesion types as described below (17). In the NAWM intact myelin is shown as intense blue staining (Fig. 3 a, d). The distribution of active astrocytes was rather sparse (Fig. 3 b, e), the single astrocytes were clearly separated from each other. A normal OPC distribution (represented by dark dots in the tissue) and a normal PLP immunoreactivity is shown in figure 3 c and f. Active (A) lesions appeared pink in LFB and are characterized by the presence of early (blue) myelin

degradation products in macrophages within the lesion (Fig. 3 g). In comparison to the NAWM astrocytes in A lesions already appeared larger and more branched (Fig. 3 h).

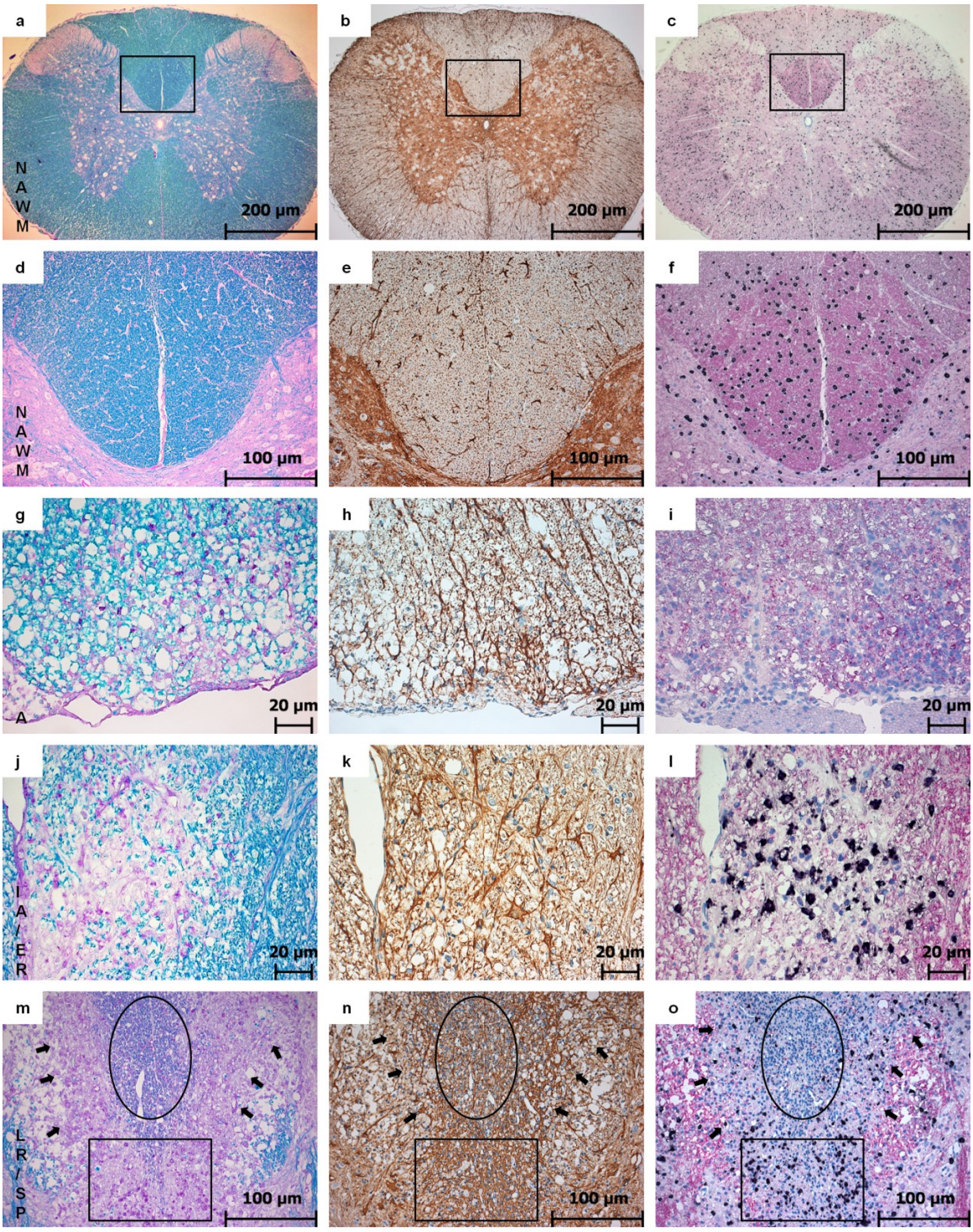

Figure 3: Lesion evolution in the rat spinal cord. This figure shows the results of LFB over the course of lesion evolution (first row; a, d, g, j, m). In this staining lesion areas can be detected as an overview in pink and SPs are represented in pale blue due to thinner myelin sheaths after remyelination. GFAP-IHC (second row; b, e, h, k, n) shows reactive astrocytes (dark brown) and is used to trace astrogliosis. PLP-ISH (third row; c, f, i, l, o) shows OPC density via PLP mRNA in situ hybridization (black) and the corresponding protein (in

pink) at the same time. The rectangles in the figures of the first line (a, b, c) indicate the areas in the second line at a higher magnification (d, e, f). The first and the second line show the NAWM with normal, dark blue myelin in LFB (a, d), only some active astrocytes in GFAP (b, e) and a normal distribution of OPCs with a strong PLP immunoreactivity (c, f). In A pink areas represent the absent myelin in LFB; macrophages are carrying early (blue) myelin degradation products (g). Astrocytes are more activated and start to branch (h), OPCs are nearly absent and PLP loss is indicated by a pale pink area (j). IA/ER clearly set apart in pink in LFB and myelin degradation products are already digested and appear in pink as well (j). Astrocytes are getting even larger and more branched (k) and a massive accumulation of OPCs can be observed in the same area where PLP loss is detectable (l). Lesions tend to undergo smooth transition between different stages with different lesion types bordering (m-o). The circle marks the SP area in LFB (m), GFAP (n) and PLP (o). The rectangle indicates a part with ongoing ER and the arrows point at the border of LR. Reproduced from (17) with permission of the publisher (Wiley).

As expected for an active demyelination there was no ongoing remyelination detectable, which was indicated by a total loss of OPCs in the lesion area (Fig. 3 i). The associated PLP additionally appeared thinned out discernible by the pale pink background (Fig. 3 i). In IA/ER (Fig. 3 j-l) the demyelinated area still appeared in pink in LFB staining (Fig. 3 j) with macrophages containing late (pink) myelin degradation products whereas the astrocytic network on an adjacent slide of the same lesion was already getting more dense (Fig. 3 k). The glial reaction coexisted with marked ongoing remyelination. The highest number of OPCs could be found in IA/ER lesions, while the pale pink PLP immunoreactivity indicated substantial loss of PLP (Fig. 3 l). Especially in later lesions stages smooth lesion type transitions within one large lesion are most common in this experimental model with one large lesion containing edges of different stages of de- and remyelination. The rectangle in figure 3 m-o represents an IA/ER area with macrophages appearing with pink myelin degradation products in LFB staining (Fig. 3 m), slightly branched, activated astrocytes (Fig. 3 n) and a very high number of OPCs (Fig. 3 o). The arrows in figure 3 m-o are pointing at the LR border represented in LFB as a pink rim (Fig. 3 m), in GFAP staining as a heavily branched astrocytic network (Fig. 3 n) and with a decreasing OPC occurrence (Fig. 3 o). The circle in figure 3 m-o indicates the SP area, embedded in a rim of IA/ER and LR lesions. In LFB this area appeared light blue (Fig. 3 m) and in GFAP staining a very dense network represented the glial scar (Fig. 3 n). The massive counterstain indicated by the high amount of blue nuclei is one of the typical signs – some astrocytes have more than one nucleus in this lesion state. The OPC distribution approximated to those found in the NAWM (Fig. 3 o) with PLP staining still pale (17).

Quantitative assessment of astrogliosis and oligodendrocytes

GFAP immunoreactivity was assessed in a total of 540 spinal cord lesions; in 450 lesions the number of OPCs was quantified and for evaluation of mature oligodendrocytes we used a selected set of 120 representative lesions. Table 1 lists the total number of assessed lesions and the corresponding number of rats (17).

Table 1: Number of quantified lesions for GFAP-IHC, PLP-ISH and NOGO-IHC.

	NAWM	A	IA/ER	ER/LR	LR/SP	SP	Total	Rats
GFAP-IHC	77	116	84	88	90	85	540	45
PLP-ISH	61	70	76	79	85	79	450	45
NOGO-IHC	20	20	20	20	20	20	120	15

In total, GFAP immunoreactivity (GFAP-IHC) was assessed in 540 lesions OPC density (PLP-ISH) in 450 lesions and occurrence of mature Oligodendrocytes (NOGO-IHC) in 120 lesions by one blinded investigator (MTH). Reproduced from (17) with permission of the publisher (Wiley).

The results of the quantitative evaluation of GFAP positive astrocytes, representing the development of the glial scar, PLP mRNA positive OPCs as markers of remyelination in the different lesion types and NOGO positive cells as marker for mature oligodendrocytes of rat spinal cords are shown in box plots in figure 4 a, b and c, respectively. The corresponding number with median and percentiles are given in supplementary table 3 (17). With ongoing lesion evolution the number of GFAP expressing astrocytes increased steadily from a median of 200 cells/mm^2 in A lesions to SP with a peak of 4500 cells/mm^2, representing all features of a glial scar. All lesion types differed significantly from each other and NAWM in respect to the detected number of GFAP positive astrocytes ($p < 0.001$). The quantitative assessment of the glial scar formation can be followed in figure 4 a (17).

Active demyelination was associated with a loss of remyelinating and protecting cells indicated by a sharp drop of OPCs as compared to NAWM (median of 587 cells/mm^2) to A (with a median of 20 cells/mm^2). At the beginning of remyelination there was an increase of OPCs detectable with a median of 1479 cells/mm^2 ($p < 0.001$). The median of detected PLP mRNA expressing OPCs in ER/LR, LR/SP and SP was between 614 and 750 cells/mm^2, which is close to the number of OPCs detectable in NAWM (p-values NAWM to ER/LR = 0.157, NAWM to LR/SP = 0.185 and NAWM to SP = 0.893). The number of PLP mRNA expressing OPCs in ER/LR was slightly higher than in LR/SP ($p = 0.223$) and a decrease from ER/LR to SP ($p = 0.175$) could be observed but these differences did not reach statistical significance. The quantitative evaluation of PLP mRNA expression of each lesion type is represented in a box plot in figure 4 b. Beside the loss of OPCs during

active demyelination also a drop of mature oligodendrocytes could be seen from NAWM (median of 308 cells/mm^2) to A (median of 67 cells/mm^2; ($p < 0.001$). During early remyelination there was also an increase of mature oligodendrocytes detectable (median 476 cells/mm^2). Most mature oligodendrocytes were found during early to late remyelination with a median of 645 cells/mm^2. The number of cells decreased again during late remyelination to a number comparable to early remyelination (median 497 cells/mm^2). In fully remyelinated SP the number of mature oligodendrocytes was comparable to that in NAWM with a median of 328 cells/mm^2. The quantitative evaluation of NOGO-IHC during lesion evolution is shown in a box plot in figure 4 c (17).

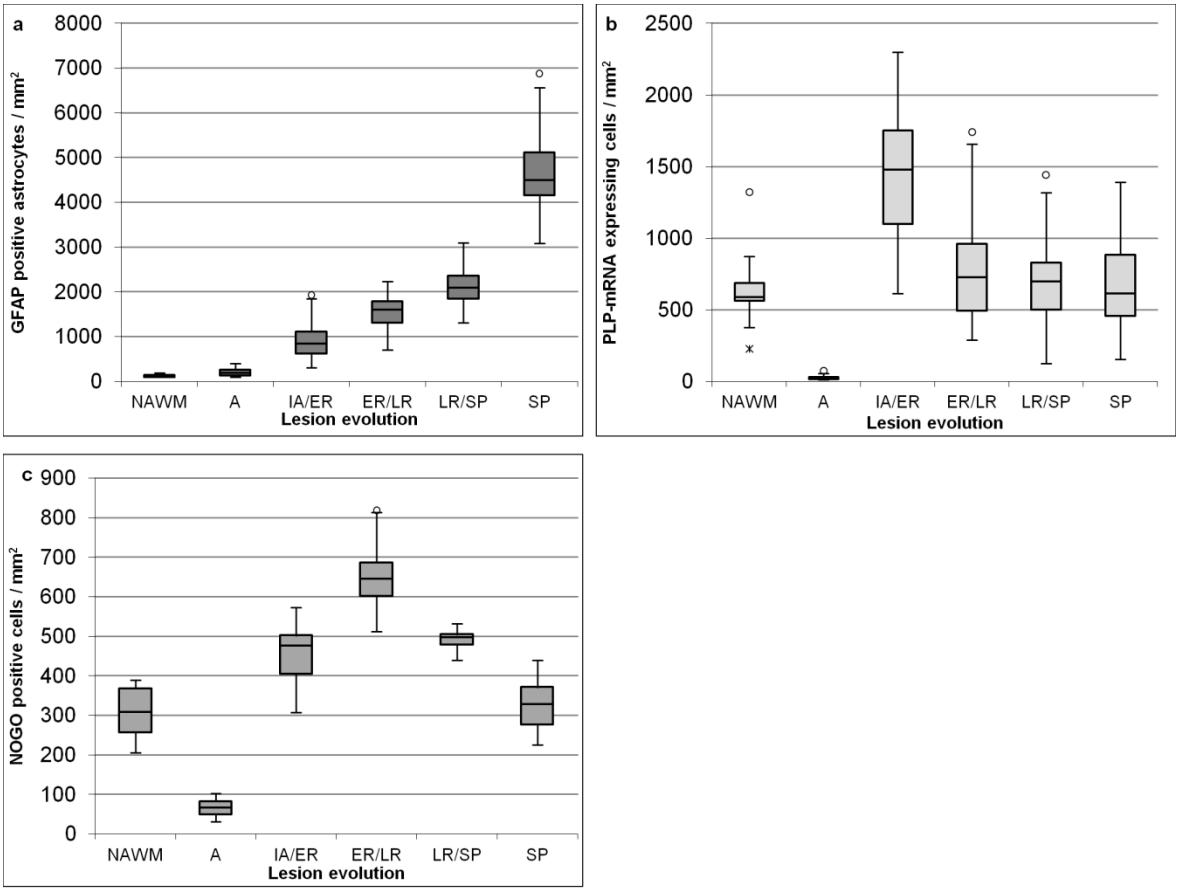

Figure 4: Quantification of GFAP positive astrocytes, PLP mRNA expressing OPCs and NOGO positive mature oligodendrocytes. Astrogliosis as a marker of diseased tissue increases during lesion evolution and reaches its peak in SP representing all features known for a glial scar (a). In NAWM only a few astrocytes are GFAP positive and a significant upregulation of GFAP expressing astrocytes is detectable in SP with almost all astrocytes expressing GFAP. All groups differ significantly from each other ($p < 0.001$). In total 540 lesions were quantified for GFAP (out of 45 rats). The observation of OPCs during lesion evolution reveals in a peak of PLP mRNA expression in IA/ER (b). Hardly any OPCs were expressing PLP mRNA in A. PLP mRNA expression in fully remyelinated SP shows close resemblance to the expression in NAWM. ER/LR and LR/SP results are slightly over the range of detected OPCs in NAWM and SP. Only A and IA/ER lesions differ significantly from the other groups ($p < 0.001$). In total 450 lesions were quantified for PLP (out of 45 rats). As expected the distribution of NOGO-positive cells (mature oligodendrocytes) follow the course of OPCs with a

slight delay. During A mature oligodendrocytes are comparably low. There is an increase of mature oligodendrocytes detectable during early remyelination indicating a successful differentiation of OPCs. Mature oligodendrocytes are also detectable during late remyelination and their occurrence in SP is comparable with their appearance in NAWM. All groups differ significantly from each other ($p < 0.01$) with the exception of NAWM to SP ($p = 0.541$) and IA/ER to ER/LR ($p = 0.086$). In total 120 lesions were quantified for NOGO (out of 15 rats). Reproduced from (17) with permission of the publisher (Wiley).

Astrocyte-derived factors

To further investigate the role of astrocytes and the plaque milieu in the different lesion types we traced a set of astrocyte-derived factors known for their involvement during lesion evolution and remyelination via IHC double staining of GFAP and the respective factor. For displaying the corresponding ratio of astrocytes expressing the respective factors we chose a percentage scale. The selected set of astrocytic factors was quantitatively assessed in all different lesion types on representative slides ($n = 20$ per factor and lesion type). As already mentioned above we encountered all investigated factors in all lesion types with different patterns of distribution (Fig. 5). Some factors exhibited only small changes during lesion evolution; others underwent a remarkable change in expression pattern along the lesion evolution and the ongoing remyelination process. We arranged the factors according to their peak occurrence during lesion evolution and discuss the results systematically over the full course of lesion evolution (17).

During active demyelination we found Sema3A, Sema3F, HABP and BMP-2 to be highly up-regulated (Fig. 5 a-d). In this stage recruitment of OPCs already starts. We could detect a higher expression of Sema3A with 63% in this lesion type whereas only about 50% of astrocytes were expressing Sema3F. Interestingly Sema3A was also very present in LR/SP (57%) and Sema3F in ER/LR (69%). HABP was highly expressed in active lesions by up to 80% of all detected astrocytes and BMP-2 was very present during active demyelination with almost 85% of all astrocytes being BMP-2 positive. BMP-2 was also very highly expressed during LR (17). For successful ER migration of OPCs to inactive lesions is necessary. Important factors highly expressed during this step in our sample were CNTF and BDNF (Fig. 5 e and f). CNTF peaked during ER with about 70% of all astrocytes expressing it and then decreased again during later phases of remyelination. BDNF only slightly increased during ER and was also present during active demyelination (17). It is important for OPCs to be able to survive and differentiate in the lesion milieu during remyelination. In ER/LR lesions we found CXCL-12, FN1 and Tn-C to be highly up-regulated (Fig. 5 g-i). CXCL-12 increased during remyelination to a maximum of 80% in ER/LR. Upon completion of remyelination their number decreased to 8% in the shadow

plaque. More than 40% of all astrocytes were expressing FN1 during ER/LR but this factor was also comparable high during active demyelination and LR/SP lesions. Tn-C increased during ER/LR up to almost 60% and was also high during active demyelination and LR/SP (17). During LR/SP we found IGF to be highly expressed with almost 70% of all astrocytes being positive (Fig. 5 j) followed by a remarkable decrease to 21% upon reaching the SP (17).

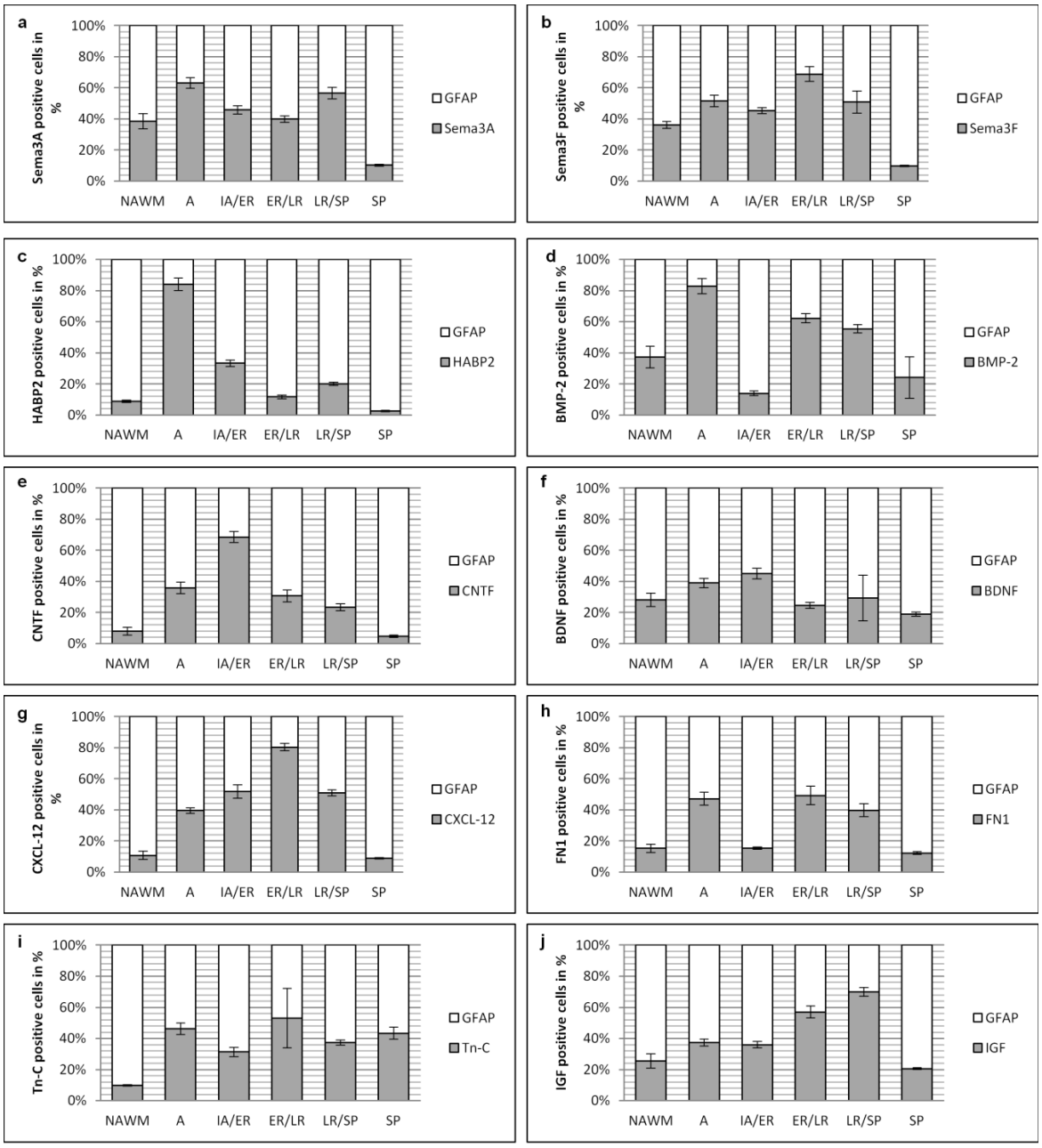

Figure 5: Percent scale of GFAP positive astrocytes and astrocyte-derived factors on selected spinal cord lesions. In each lesion the mean of all astrocytes represents the 100% scale and the corresponding astrocytes expressing factors involved in OPC regulation are given in the appropriate ratios (selected lesions n = 20 per factor). Error bars represent 95% CI. The guidance molecule Sema3A (a) peaks in A with more than 60% of active astrocytes expressing this factor and additionally shows a high occurrence in LR/SP with

approximately 55%. In A the expression of Sema3F (b) is higher than in IA/ER and peaks again in ER/LR. HABP2 (c) is highly present during A with more than 80% of all astrocytes expressing this factor. It decreases again to 5-30% during remyelination. BMP-2 (d) is comparably high during A decreases in IA/ER and increases again during later remyelination steps. CNTF expression (e) increases during lesion evolution with a peak of almost 70% CNTF positive astrocytes in IA/ER and decreases again to approximately 5% in SP. BDNF (f) expression increases from NAWM to IA/ER, decreases in ER/LR, increases again in LR/SP and reaches its minimum in SP. CXCL-12 (g) increases during lesion evolution, peaks in ER/LR with 80% of active astrocytes expressing this factor and decreases again from LR/SP to SP. Around 50% of all astrocytes are FN1 positive during A and late remyelination steps (h). Tn-C is upregulated during A and ER/LR (i). The expression of IGF (j) rises from NAWM to LR/SP with a slight increase in A and falls rapidly from LR/SP to SP. Reproduced with modifications from (17) with permission of the publisher (Wiley).

Figure 6 represents a summary of the most important results of the investigated astrocytic factors. All factors in green boxes are expressed by activated astrocytes during lesion evolution.

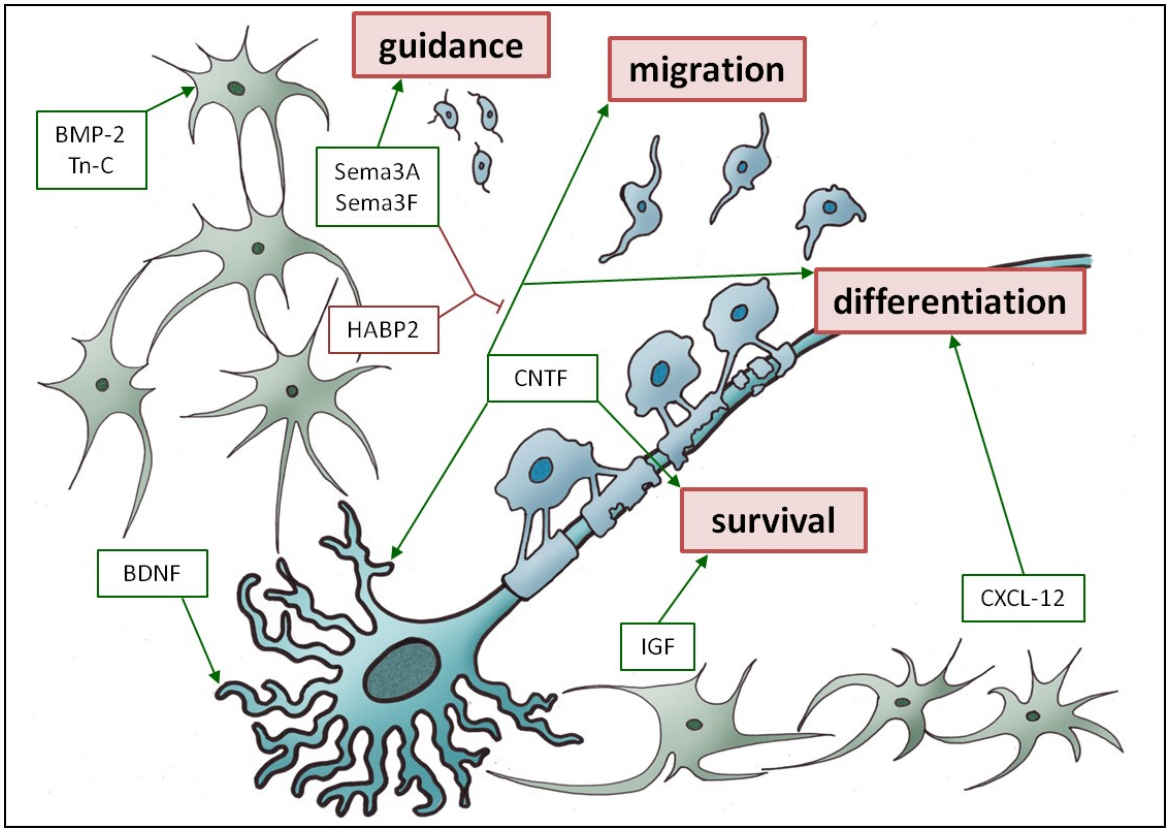

Figure 6: Summary of most important astrocytic factors described in this thesis. This scheme represents one neuron (turquoise) with some destroyed myelin sheaths (light blue). In order to repair this damage, oligodendrocytes (light blue) have to be guided to the damage, migrate, differentiate and survive in the plaque milieu. Astrocytes (green) are involved in those steps and the most important factors expressed by astrocytes and discussed in this thesis are written in green boxes. Green arrows indicate a facilitating effect of the factor and red lines indicate a prohibiting effect. Drawings and word art by Michaela Tanja Haindl.

Green arrows indicate the supportive role of the respective factor on guidance, migration, differentiation or survival of oligodendrocytes during remyelination. Astrocytes are displayed in green and oligodendrocytes in blue. There is one schematic neuron with some destroyed myelin sheaths, displayed in blue. Sema3A and Sema3F are important for OPC guidance while suppressing migration and differentiation, indicated by the red line. HABP2 is also suppressing migration and differentiation during this step. CNTF facilitates migration differentiation and survival of oligodendrocytes. Similar to BDNF it also protects nerve-cell processes. CXCL-12 is important for OPC differentiation and IGF for survival of oligodendrocytes. BMP-2 and Tn-C are supporting glial scar formation.

The switch of astrocytic phenotypes

Neuroinflammation induces two different types of reactive astrocytes that were termed A1 and A2 according to Liddelow et al 2017. A1 are described as regulating classical complement cascade genes and postulated as harmful. In contrast A2 astrocytes regulate many neurotrophic factors and are described as being protective (17,32).

In NAWM both A1 and A2 phenotypes were detectable with a twofold higher number of A2 astrocytes (83 +/- 9.8) than A1 (40 +/- 9.4). In A more than twice as much astrocytes were carrying the A1 phenotype (195 +/- 13.6) and only a moderate number carrying A2 (90 +/- 8.6). Interestingly we found almost all astrocytes being A2 (green) in IA/ER lesions (604 +/- 30.0) and the marker of A1 (red) spread over the whole lesion in a granular manner (Fig. 7 a). From ER/LR lesions to LR/SP lesions almost all astrocytes showed the A2 (purple) phenotype within the lesion with a surrounding small rim of A1 (brown) astrocytes bordering the lesion (Fig. 7 b, c). In fully remyelinated SP the majority of astrocytes showed the A2 (green) phenotype (4625 +/- 448.1) and only a few astrocytes exhibited A1 (red) characteristics (22 +/- 10.1; the circle in Fig. 7 d and e) (17).

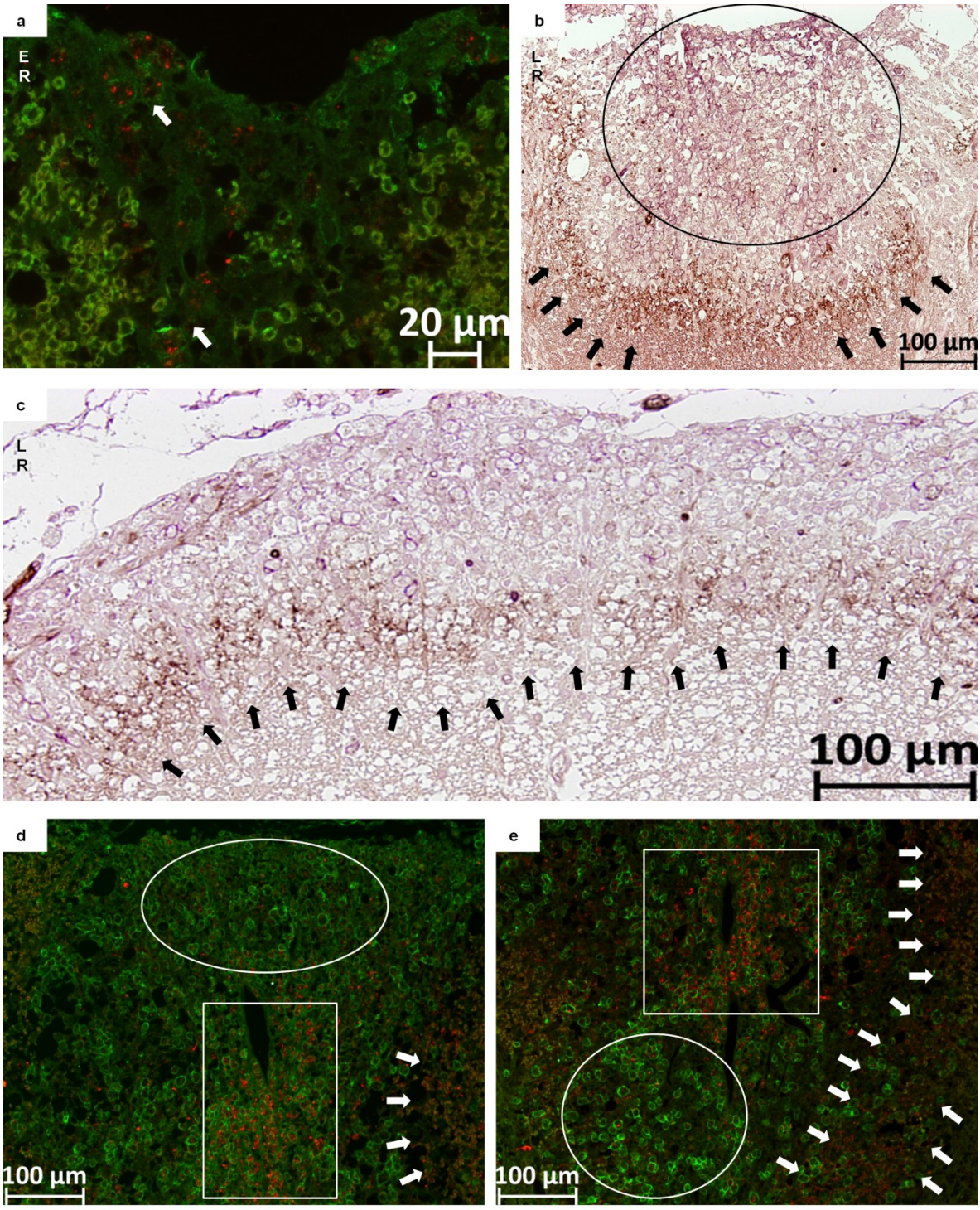

Figure 7: The switch of astrocytic phenotype A1 and A2 during lesion evolution. In all IF stainings the A1 phenotype (C3d) appears in red and the A2 phenotype (S100A10) in green. In all IHC stainings the A1 phenotype appears in brown and the A2 phenotype in purple. In (a) an early remyelination lesion is shown on a IF stained slide where the A2 phenotype is mainly present and the A1 phenotype is spread over the lesion in a granular like pattern indicated by the arrows. In (b) an IHC of a late remyelination lesion is marked by the circle where the A2 phenotype (purple) is mainly present. The arrows point at the lesion border where the A1 phenotype (brown) accumulates. This remarkable border is also shown in another late remyelination lesion in (c) indicated by the arrows. In (d) and (e) IF stainings are shown with different lesion types side by side. The circles show SPs where the A2 phenotype (green) is mainly present. In the rectangles early remyelination

areas are marked with the A1 phenotype (red) spread over in a granular like pattern. The arrows show the border of A1 phenotype, which was detectable during later remyelination steps in our sample. Reproduced from (17) with permission of the publisher (Wiley).

CLM results

Histopathological changes in the rat cortex

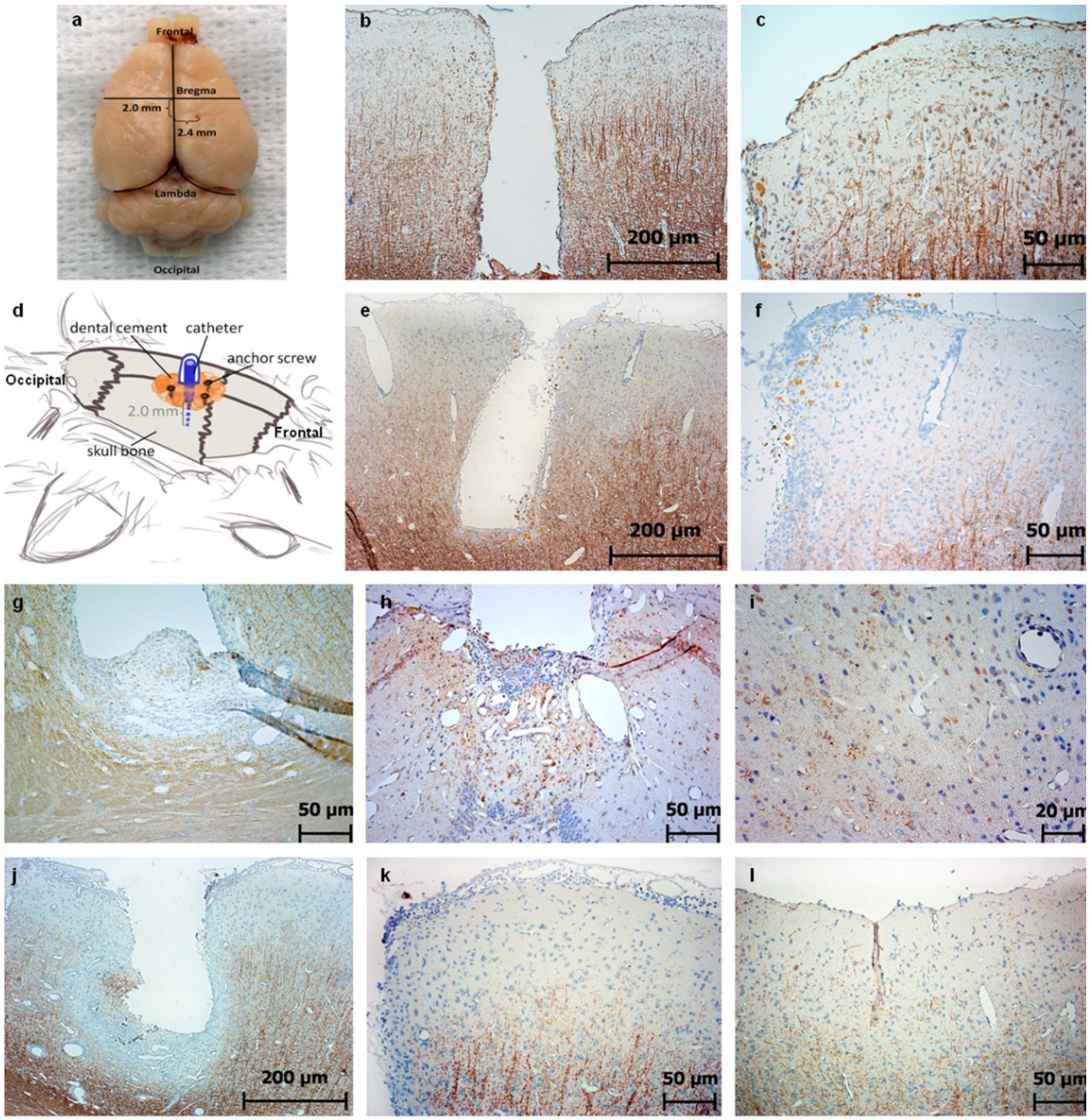

Figure 8: Implantation setup and histological tissue changes on day 1 and 3 after cytokine injection. The basic catheter implantation setup according to the coordinates 2 mm posterior to the bregma and 2.4 mm to the right is shown in (a). The catheter is then placed in a depth of 2 mm. A scheme of the full catheter setup is shown in (d) with three anchor screws and dental cement. A tissue section of a control animal (b) and (c) shows healthy conditions of PLP reactivity (IHC against PLP). In (e) and (f) the cone shaped loss of PLP immunoreactivity in the immediate catheter implantation area in MOG immunized animals on day 1 after cytokine injection is shown. The PLP loss below the catheter tip close to the corpus callosum, affecting partly

also the white matter is shown in (g). Complement deposits (C9neo) are found in traces around small blood vessels on day 1 as well, shown in (h) and (i). On day 3 after cytokine injection PLP loss extends to larger areas of the injected hemisphere (j), (k). Furthermore a slight PLP loss can also be detected in the contralateral hemisphere in a small area right beneath one of the anchor screws (l). Reproduced with modifications from (18) with permission of the publisher (Elsevier).

Loss of cortical PLP immunoreactivity

In MOG-primed animals loss of PLP immunoreactivity was detectable starting on day 1 after injection of the cytokines. Figure 8 a and figure 8 (a and d) show the coordinates and a scheme of catheter implantation to illustrate where the following microscopic pictures are located. Normal PLP immunoreactivity of a control animal (which was fully immunized but received an injection of sterile PBS on day 1 only without cytokines) is shown in figure 8 b and c. On day 1 after cytokine injection demyelination was restricted to the immediate catheter area and extended from the tip of the catheter towards subpial areas in a cone-like pattern in the injected hemisphere (Fig. 8 e and f). To a much lesser extent demyelination affected also the white matter of the corpus callosum just below the catheter tip right at the border to the cortex (as shown in Fig. 8 g). The contralateral hemisphere showed normal PLP immunoreactivity. On day 3 after cytokine injection demyelination was already much more pronounced at the catheter site (Fig. 8 j and k) and had also spread to the contralateral hemisphere in the area beneath one of the anchor crews (Fig. 8 l) (18).

Cortical demyelination was most pronounced on day 15 after cytokine injection, where it included large parts of the cortex of both hemispheres (Fig. 9a shows an overview over both hemispheres, Fig. 9 b, c the loss of PLP immunoreactivity in the catheter area and Fig. 9 d in the contralateral hemisphere). On day 30 PLP reactivity was partially restored again but patches of still missing or thinned out myelin had remained in both hemispheres in subpial and intracortical areas (Fig. 9 e-i). The induction of a second relapse on day 30 led to a stabilization or even slight increase of the extent of the demyelinated cortical area, obviously counteracting remyelination. Brains of these animals appeared atrophic (Fig. 9 k) as compared to controls (Fig. 9 j) (18).

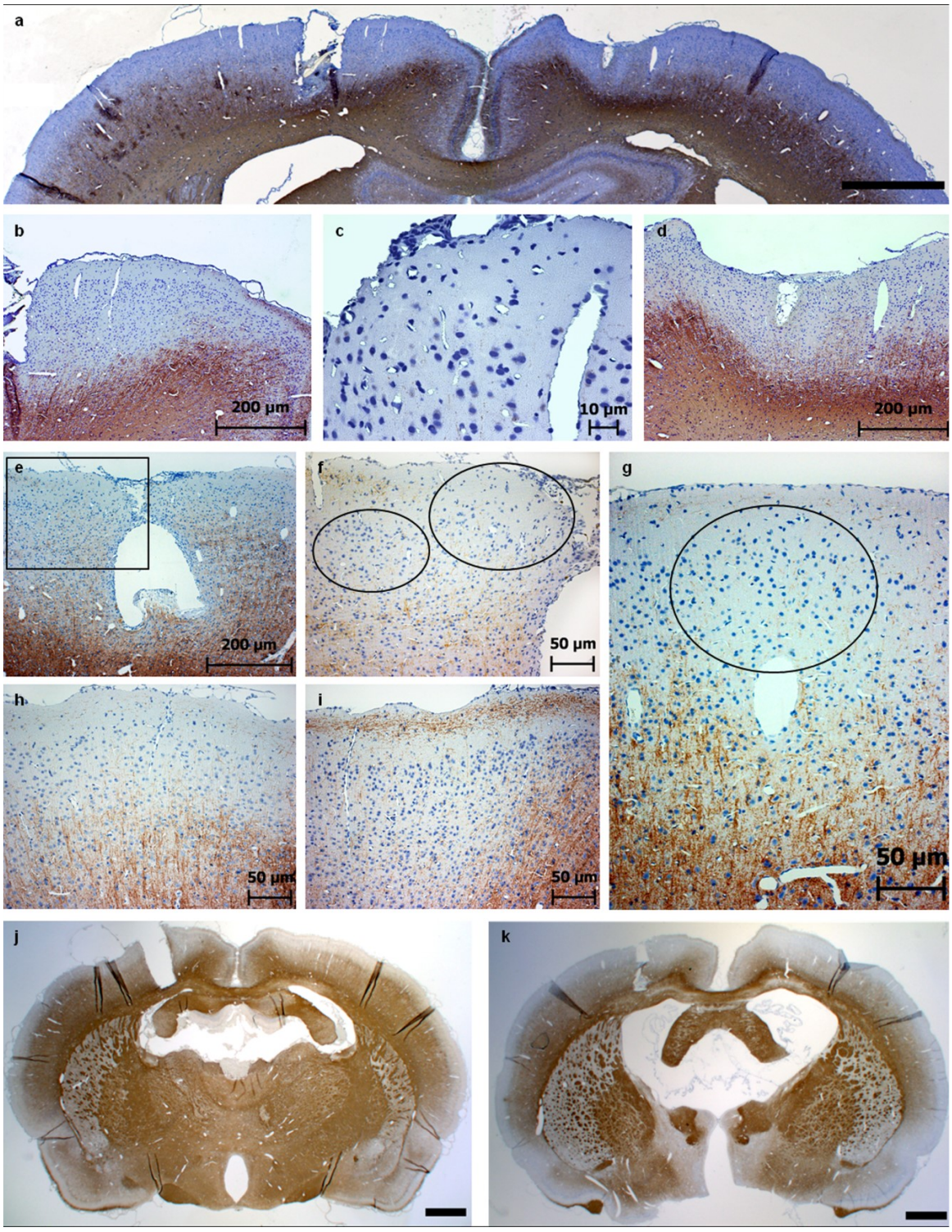

Figure 9: PLP loss is most pronounced on day 15 and still detectable on day 30 after cytokine injection. On day 15 after cytokine injection rats exhibited a widespread cortical demyelination over both hemispheres shown in (a). In (b) the catheter area is shown and the right corner is displayed in (c) at a higher magnification. There is complete loss of PLP immunoreactivity with not even residual traces detectable. PLP loss in the contralateral hemisphere is shown in (d). Histological results of day 30 after cytokine injection is shown in (e) – (g). The area in the rectangle is shown at a higher magnification in (f). The circles show still missing PLP Intracortically (left circle) and subpially (right circle) next to partially remyelinated thinned out myelin below. Also different cortical areas in the contralateral hemisphere showed both subpially (g), (h) and

intracortically (i) still missing PLP. Brains of animals sacrificed on day 15 after a second cytokine injection appeared atrophic (k) when compared to control brains (j). Reproduced from (18) with permission of the publisher (Elsevier).

Similarity to human cortical lesions

In figure 10 the close resemblance of human cortical demyelination (in this case taken from autopsy material from a fulminant MOG encephalitis) to our animal model is demonstrated.

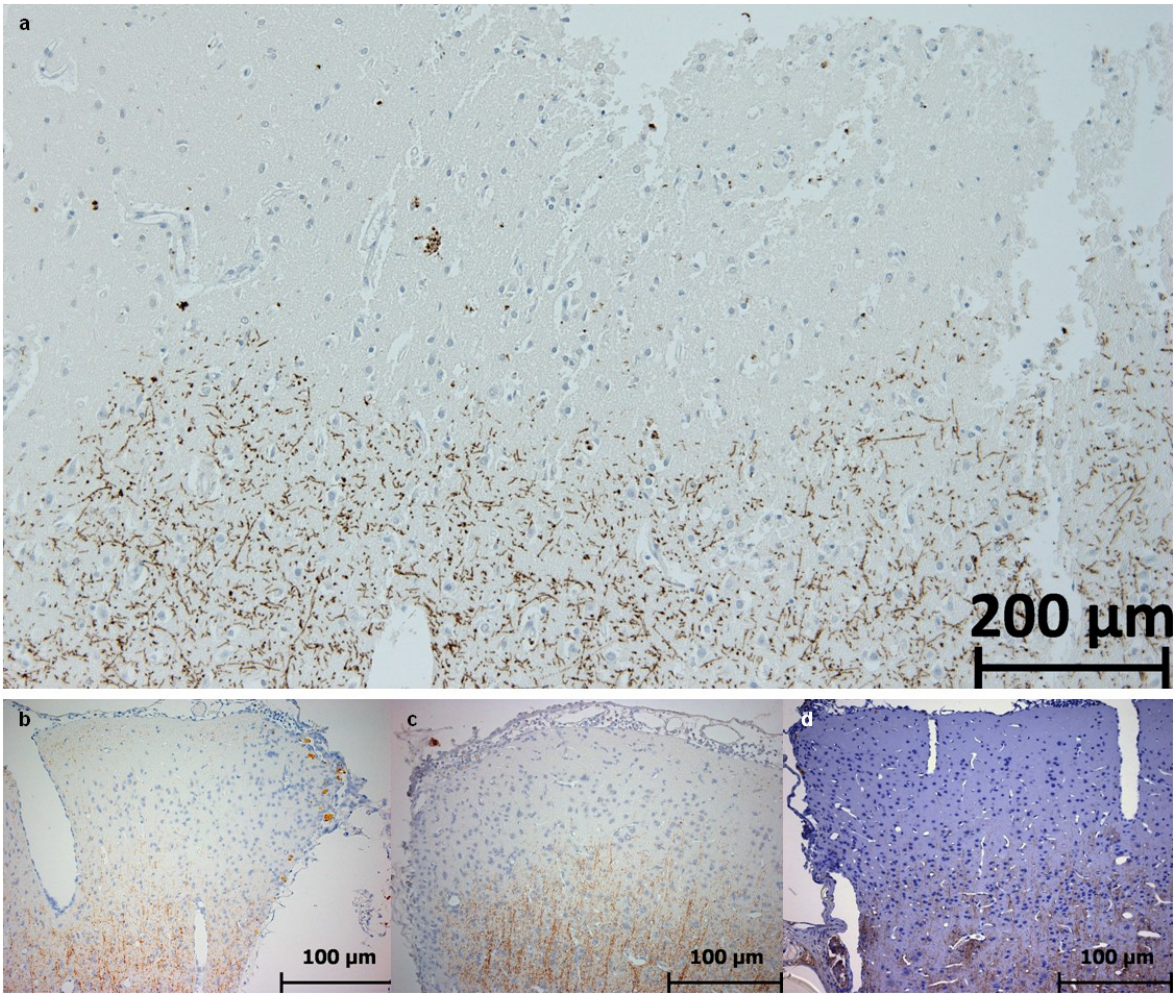

Figure 10: Similarity of our rat model to human cortical pathology, comparison of PLP stainings. In (a) a small edge of a massive cortical demyelination of a human brain is shown. In comparison (b) to (d) shows the catheter edge of our animal model on day 1 (b), day 3 (c) and day 15 (d). In all 4 pictures only few PLP residues are left. Note, that (d) only appears in strong blue because of the stronger counter stain. Image (c) is also part of picture panel 6 (k).

Figure 10 (a) shows the edge of a human cortical lesion in PLP staining with almost all PLP gone in the upper cortex area. In comparison our animal model shows a cortical pathology looking pretty much the same starting on day 1 (Fig. 10 b) with only a small

comparable area, on day 3 where cortical pathology starts to expand (Fig. 10 c) and on day 15 with widespread cortical demyelination (d, only a small part is shown here).

Microglia activation

Cortical PLP loss was accompanied by microglia activation in both hemispheres, which was more pronounced in the ipsilateral hemisphere throughout the disease course (Fig. 11). Figure 11 shows a confocal double staining for activated microglia (Iba1, green) and PLP (red) of a healthy control animal (Fig. 11 a) and on day 15 after cytokine injection (Fig. 11 b). There are only minor traces of remaining PLP immunoreactivity, but marked microglia activation is seen in the affected cortical area (18).

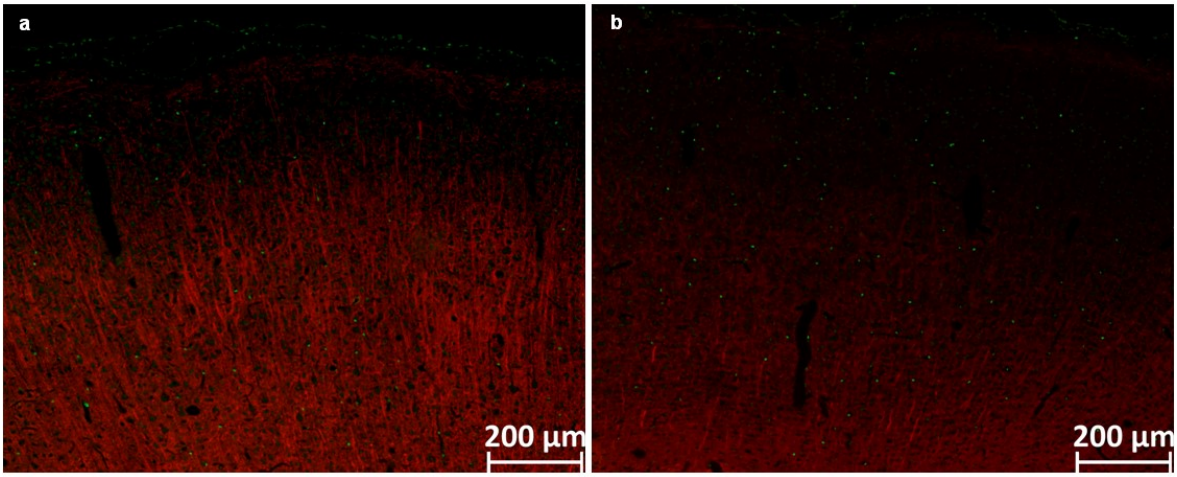

Figure 11: Microglial activation (green) and PLP loss (red) of the contralateral side - comparison of tissue sections of a control animal (a) and an animal at day 15 after cytokine injection (b). There is a normal PLP occurrence in the tissue section of the control animal (a) and normal, moderate microglial activation. In comparison (b) shows a tissue section of a day 15 animal with remarkable loss of PLP and upregulated microglial activation. Note, that the upper cortex in (b) nearly fades away under the microscope light exposure because of the very weak remaining PLP signal.

Astrocytic reaction around the catheter

In comparison to the control groups with only minor astrocytic reaction (Fig. 12 a-d), in the experimental group a marked astrocytic reaction was detectable around the catheter tip between days 1-3 after cytokine injection (Fig. 12 e, f). This reaction decreased again by days 15-30 (Fig. 12 g, h) (18).

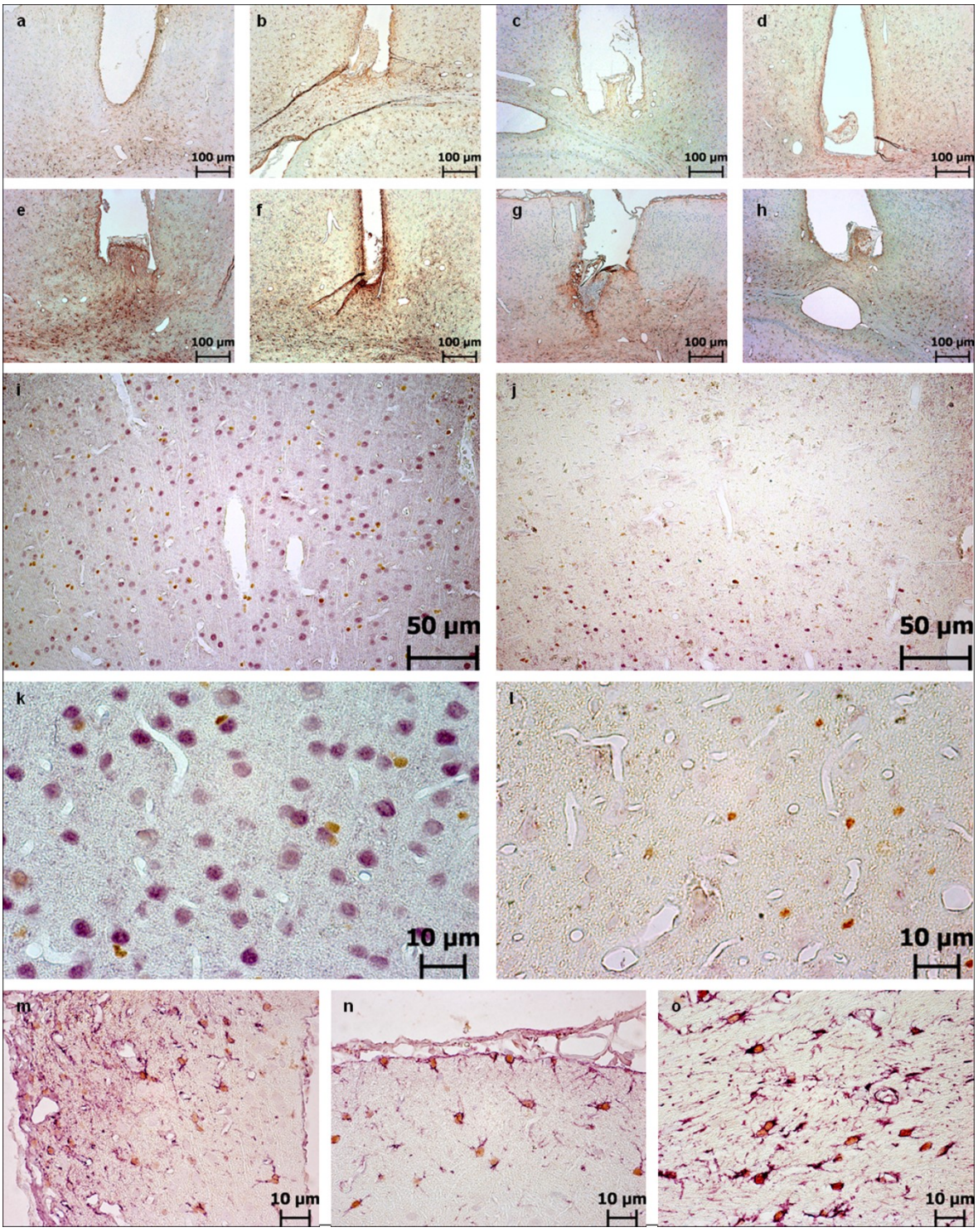

Figure 12: Astrocytic reactions around the catheter implantation site and apoptotic activity. (a) – (h) show the astrocytic reaction around the catheter implantation site in different experimental setups and time points (immunohistochemistry for GFAP). Only minor GFAP reactivity could be found in different control groups (a) – (d). (a) shows a tissue section of an animal four weeks after catheter implantation only without additional treatment or injection. Images (b) and (c) show tissue sections of animals receiving cytokine injection without previous immunization, (b) on day 1, (c) on day 3 after cytokine injection. The tissue section shown in (d) was an animal immunized with MOG but received an injection of sterile PBS through the catheter only (day 3). Images (i) – (l) show all double stainings of caspase3 (apoptosis, brown) and NeuN (neurons,

purple). (i) gives an overview of a cortex area in tissue section of an animal on day 1 after cytokine injection with still normal neuronal counts, while in (j) a cortex area of an animal on day 30 after cytokine injection with a markedly reduced neuronal count is shown. In most cases, caspase3 and NeuN seem not to co-localize, (k) and (j) show tissue sections of an animal on day 3 with at least some caspase3 positive neurons. Images (m) – (o) show double stainings of caspase3 (apoptosis, brown) and GFAP (astrocytes, purple). By far the majority of caspase3 positive cells appear to be astrocytes, as shown in (m) on day 1 close to the catheter site, in (n) on day 3 and in (o) on day 15 after a second cytokine injection. Reproduced from (18) with permission of the publisher (Elsevier).

Neuronal counts are reduced by day 15

We furthermore investigated the integrity of neurons over the disease course through immunohistochemistry against NeuN. The number of apoptotic cells was assessed through immunohistochemistry against Caspase3 during lesion evolution. A significant increase of Caspase3-positive cells could be detected on day 1 and 3 in both hemispheres, indicating most likely a direct effect of the cytokine injection in immunized animals.

Caspase3 counts then dropped by day 15 to control levels and increased again in animals sacrificed on day 30 and on day 15 after a second cytokine injection, most likely representing a delayed ongoing apoptotic activity (18). NeuN und Caspase3 double-staining however revealed only occasional occurrence of apoptotic neurons (Fig. 12 i-l, Caspase3 shown in brown, NeuN in purple). By far most of the apoptotic cells seem to represent astrocytes (as shown in GFAP/Caspase3 double stainings in Fig. 12 m-o, Caspase3 marked in brown, GFAP in purple) (18).

Histopathological comparison of VitD supplemented rat tissue versus controls

On peak disease there was much more PLP left in vit D supplemented animals compared to the day 15 animal without vitD supplementation (Fig. 13 b-d). A similar result could be obtained for day 30 with much more PLP remaining in vitD supplemented animals (Fig.13 e-f). Those findings could be confirmed by statistical analysis given in figure 14.

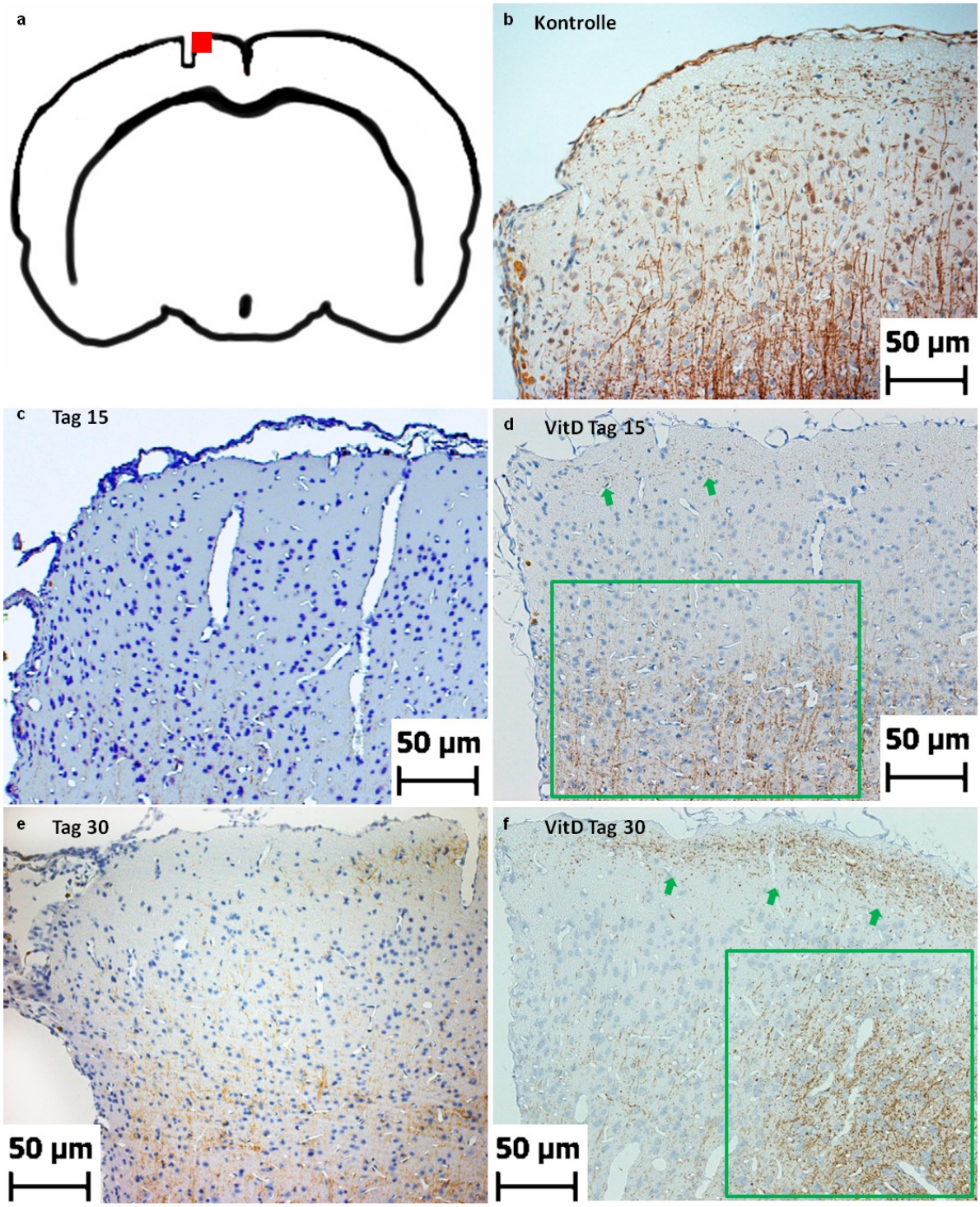

Figure 13: Histological results of vitD supplemented rats in comparison to animals without supplementation. A small scheme is shown in (a) to demonstrate where the following microscope pictures were taken. All pictures show a PLP-IHC to follow demyelination. Note, that (b), (c) and (e) are also shown in Fig. 8 and 9 to trace PLP immunoreactivity. For a better readability pairs of pictures are here compared side by side. In (b) a tissue section of a control animal is shown, comparable to the normal, healthy myelin appearance. A picture of cortical demyelination on day 15 after cytokine injection is shown in (c) where only a few thin myelin remains are detectable. In comparison (d) shows a section of a vitD supplemented animal on the same day where much more myelin is left (green rectangle and arrows). The catheter area of an

experimental animal on day 30 after cytokine injection is shown in (e). In comparison the tissue section of the vitD supplemented animal in (f) shows much more dense restored myelin (green rectangle and arrows). (b), (c), (e) Reproduced from (18) with permission of the publisher (Elsevier).

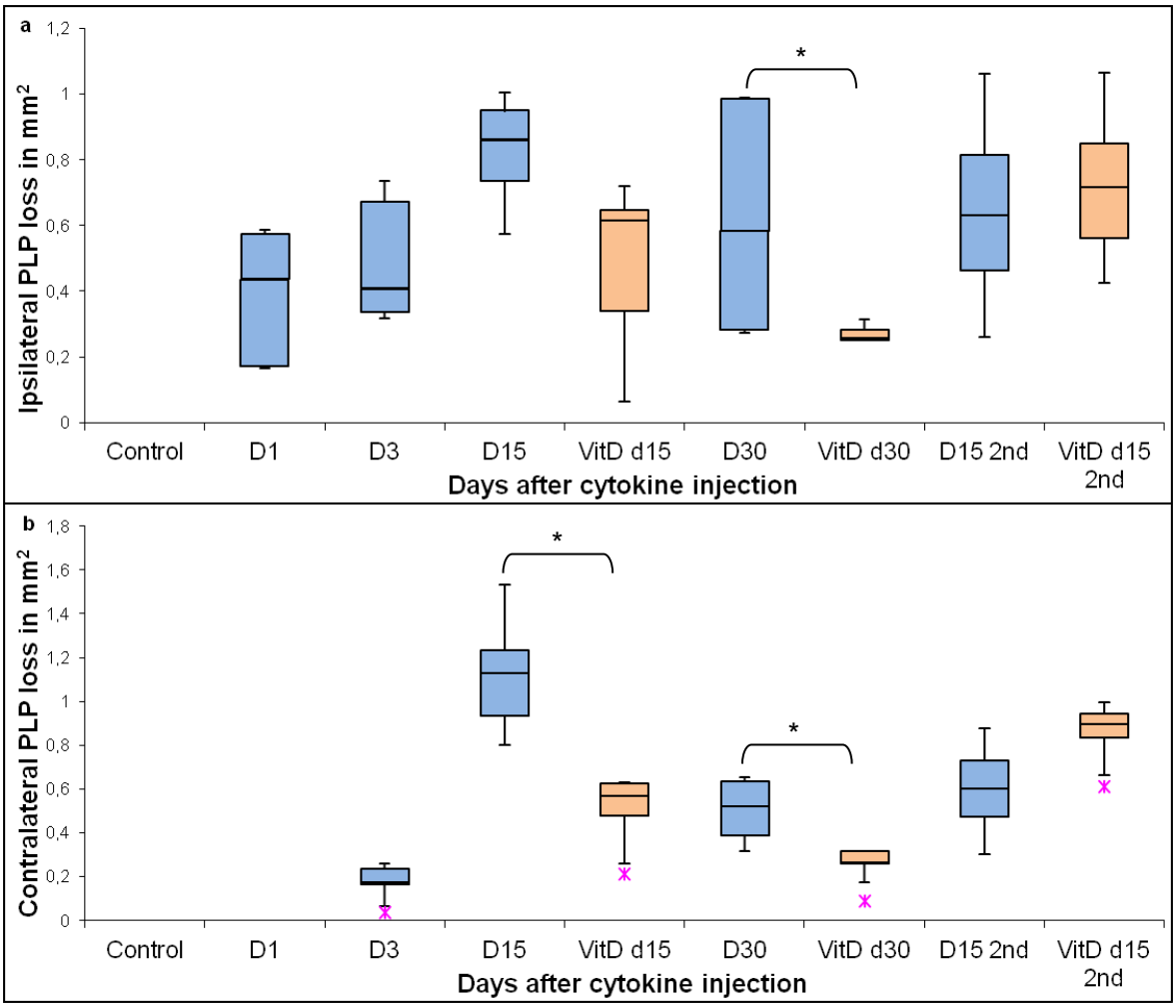

Figure 14: Quantitative evaluation of PLP loss in mm² per hemisphere. (a) shows ipsilateral results, (b) contralateral results. In the control group there was no PLP loss detectable on both hemispheres. On the ipsilateral side, PLP loss started already on day 1after cytokine injection, on the contralateral side PLP loss started on day 3. PLP loss was most pronounced on day 15. A significant reduction of PLP loss could be detected in vitD supplemented animals. On day 30 PLP was partially restored again. There was significant more PLP restored in vitD supplemented animals. On day 15 after a second cytokine injection there was again PLP loss detectable, interestingly more PLP loss in vitD supplemented animals, explainable by the difference in animal group size (n = 2 VS n = 7 vitD supplemented animals). Significant differences between experimental group and vitD supplemented groups are marked with a star.

The quantitative evaluation of cortical PLP loss over the time course and the comparison to vitD supplemented animals is given in the diagram in figure 14 (a for the ipsilateral and in b for the contralateral side). Control groups did not show any cortical PLP loss. Compared to the controls a significant PLP loss could be detected over the full course of lesion evolution with the exception of day 1, contralateral hemisphere ($p < 0.001$ in all

significant cases). Both hemispheres exhibited a significant PLP loss ($p < 0.001$) compared to the control group (18). In both hemispheres the vitD supplemented animal showed less PLP loss compared to the other experimental animals on day 15 but did only reach significance for the contralateral side (ipsilateral $p = 0.167$; contralateral $p = 0.042$). A significant difference in PLP loss between the two experimental groups on day 30 could be assessed for both hemispheres (ipsilateral $p = 0.047$; contralateral $p = 0.009$). Interestingly PLP loss was higher in vitD supplemented rats on day 15 second relapse but did not reach significance (ipsilateral $p = 0.571$; contralateral $p = 0.059$).

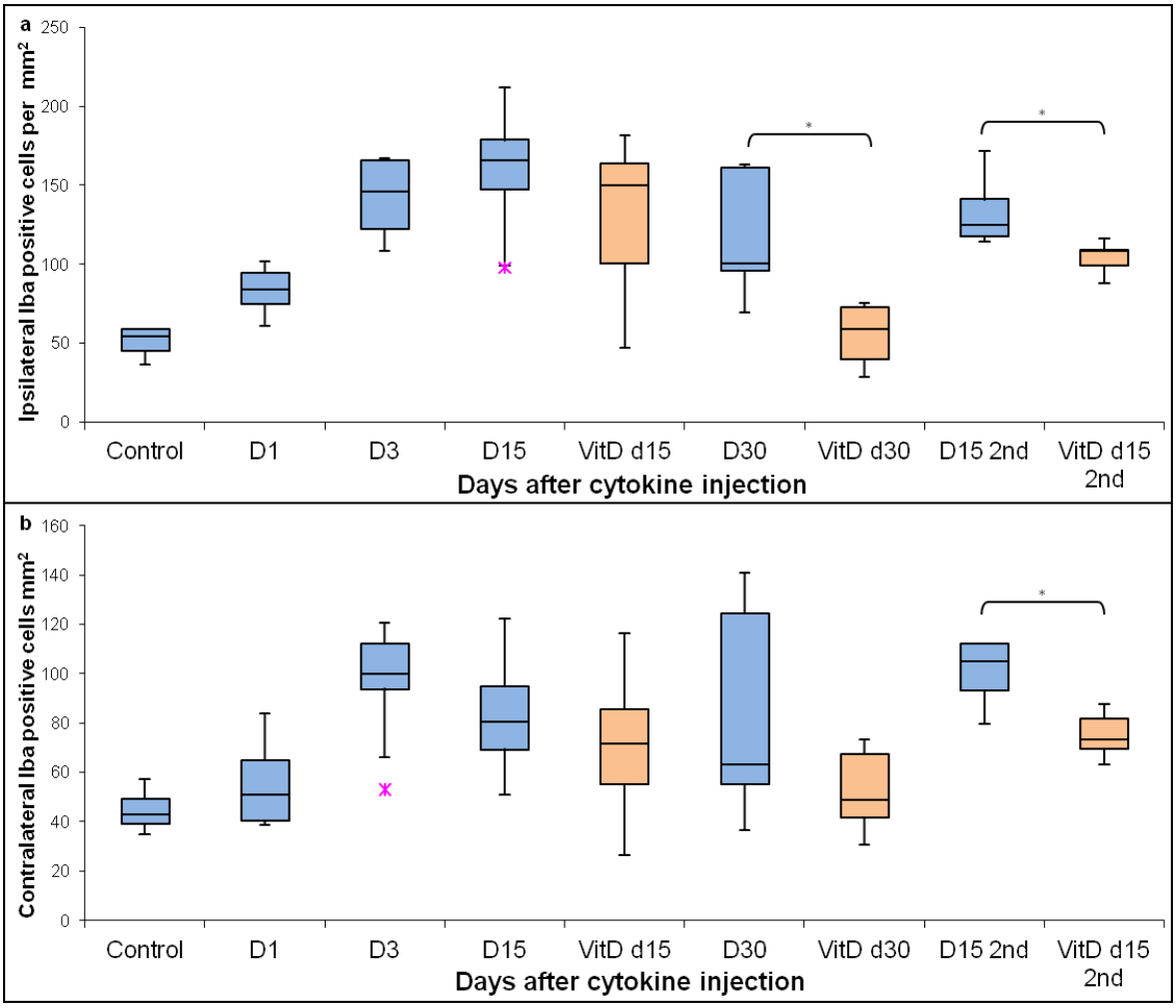

Figure 15: Quantitative evaluations of Iba positive cells in mm² per hemisphere. (a) shows ipsilateral results, (b) contralateral results. As expected microglial activation increased during the experiment and reached its maximum on day 15 ipsilateral hemisphere and day 3 contralateral hemisphere respectively. In both hemispheres vitD supplemented animals showed less microglial activation which reached significance on day 30 ipsilateral hemisphere and on day 15 second relapse on both hemispheres.

Cortical PLP loss was accompanied by microglia activation in both hemispheres, which was more pronounced in the ipsilateral hemisphere throughout the disease course (Fig. 15 a ipsilateral hemisphere, b contralateral hemisphere) and started on day 1 with a

maximum between days 3-15. In comparison to the control group the microglia activation increased significantly on all days in the ipsilateral hemisphere with p-values ranging from 0.001 to 0.003. The highest microglia activation could be detected on day 3 (p = 0.001 ipsilateral hemisphere, p = 0.002 contralateral hemisphere). Only on day 15, second relapse, the contralateral hemisphere exhibited a significant increase of microglial activity too (p = 0.008) (18). Microglial activation was upregulated during the whole experiment and was attenuated in vitD supplemented rats as displayed in figure 15. Significant less microglial activation could be detected on day 30 and day 15, second relapse of the ipsilateral hemisphere and on day 15, second relapse of the contralateral hemisphere.

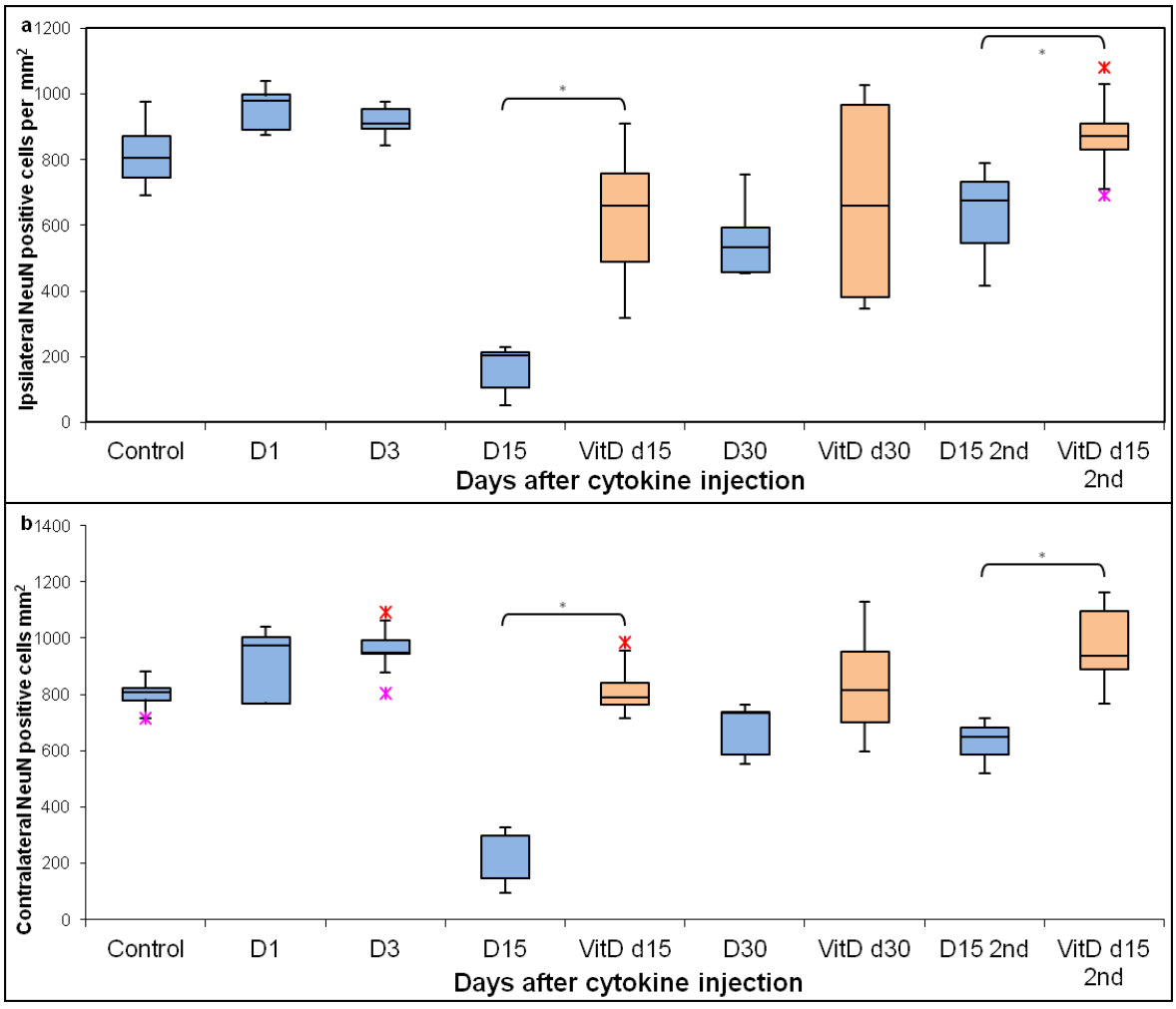

Figure 16: Quantitative evaluations of NeuN positive cells in mm² per hemisphere. (a) shows ipsilateral results, (b) contralateral results. A remarkable loss of neurons could be detected on day 15. In comparison vitD supplemented animals lost significantly less neurons on day 15 after cytokine injection. On day 30 there were also more neurons left in vitD supplemented animals but the difference did not reach significance. On day 15 after a second cytokine injection (of the same animals) there were significantly more neurons left in vitD supplemented animals compared to normal experimental conditions.

Neuronal counts remained at the level of controls on days 1-3, but then dropped significant on day 15 ($p = 0.001$ in both hemispheres). Neuronal counts remained significantly reduced compared to controls with a slight recovery of neurons on day 30 ($p = 0.002$ ipsilateral hemisphere, $p = 0.003$ contralateral hemisphere). Induction of a second demyelination phase with another cytokine injection led to a slight decrease of neuronal counts as compared to animals sacrificed on day 30 ($p = 0.008$ ipsilateral hemisphere, $p = 0.006$ in the contralateral hemisphere when compared to controls) (18). In comparison to normal experimental conditions with standard rodent food only, vitD supplemented animals did not reduce as much neurons during the whole experiment and the neuronal cell count remained at approximately the same amount from day 15 to day 15 second relapse in both hemispheres (Fig. 16 a ipsilateral hemisphere, b contralateral hemisphere).

TAC and PPm results in VitD supplemented rat serum versus controls

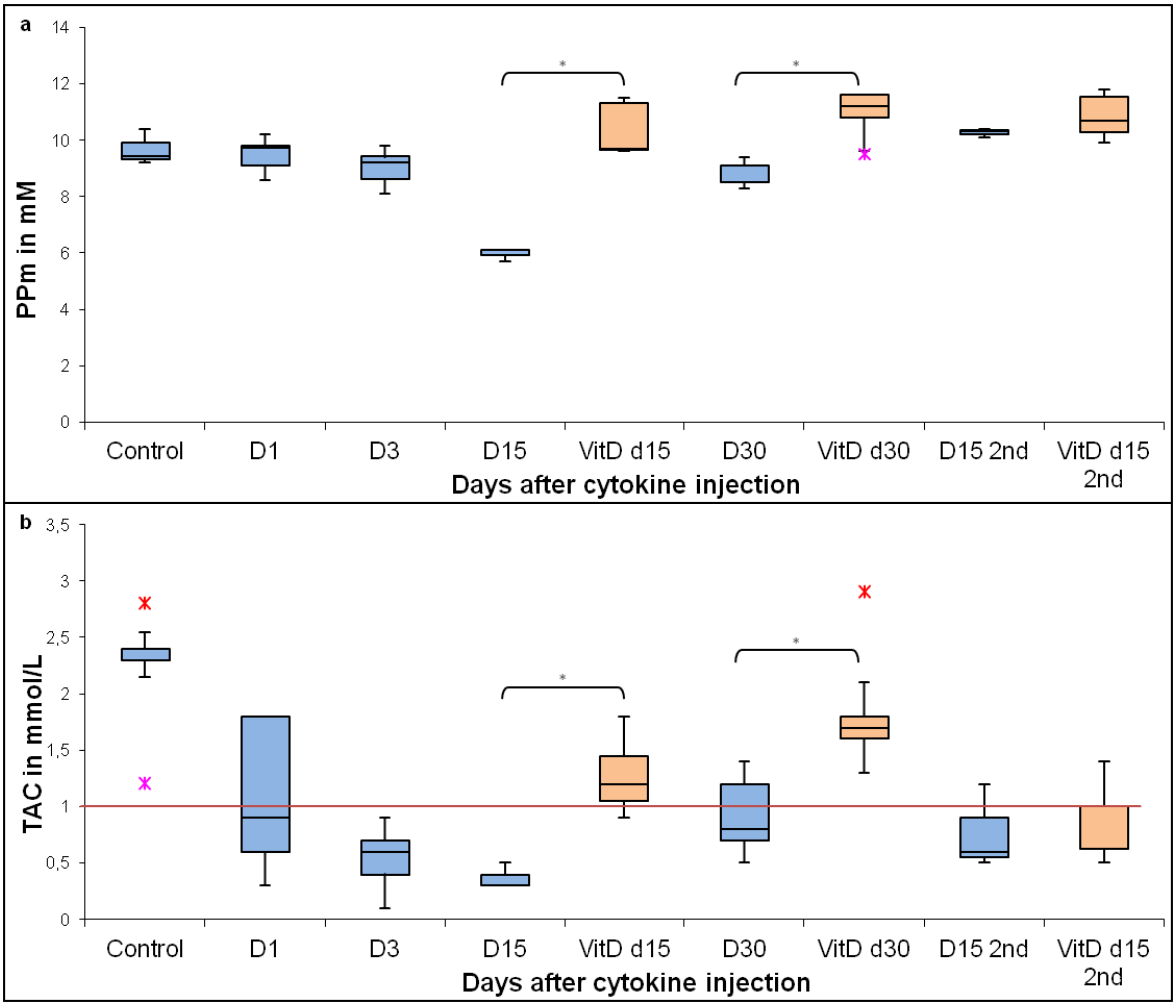

Figure 17: Results of colorimetric PPm and TAC tests. In (a) results of PPm in mM is shown. A sharp decrease of polyphenols was observed on day 15. In comparison polyphenol levels remained in the range of

healthy control animals during the whole experimental setup. PPm in vitD animals was even higher than in controls but without reaching significance. In (b) data of TAC is shown in mmol/L. The threshold value (in humans) is between 1 and 1.3 mmol/L indicated by the red line. Only healthy controls and vitD supplemented animals could reach a TAC considered as high enough. Animals subjected to the normal experimental setup without vitD supplementation showed an insufficient TAC.

A remarkable decrease of protective polyphenols was detectable on day 15 and was partially restored from day 30 to day 15, second relapse (Fig. 17 a). In comparison vitD supplemented animals showed a comparatively constant level of protective polyphenols and the amount was significantly higher on day 15 and day 30 in comparison to normal experimental conditions.

The TAC decreased beneath an insufficient threshold already on day 1 after cytokine injection and decreased further on day 15 (Fig. 17 b). On day 30 TAC was partially restored again but declined again on day 15 after a second relapse. In comparison the TAC of vitD supplemented animals was sufficient during the whole experiment and significantly higher on day 15 and day 30 in comparison to normal experimental conditions.

Discussion

In a first step I would like to discuss both, EAE and CLM results, separately. Then I will sum up all findings together and discuss the impact on neuroprotection and repair in general. Finally, this will be followed by a conclusion and discussion upon limitations of the methods and novelty value of the whole work. Suggestions for further work will finish the discussion.

EAE: the glial scar does not prohibit remyelination

Remyelination after a demyelinating event proceeds in distinct stages. Oligodendrocytes are indispensable for remyelination. Oligodendrocytes Precursor cells (OPCs) have to be recruited and migrate to the respective lesion. The next mandatory step is the differentiation of OPCs to mature oligodendrocytes. Finally OPCs must be able to survive and proliferate in the plaque milieu (17). Depending on their activation state astrocytes can exert both remyelination facilitating and potent suppressive effects on OPCs (17,20,21,35). In our work we show, that astrogliosis increases over the time course of lesion evolution. The shadow plaque represents at the same time all characteristics of a glial scar, which should - according to the literature - prevent OPCs from entering the tissue and counteract remyelination. The number of OPCs however is similar to those found in NAWM indicating that OPCs must be able to accomplish remyelination (17). We could even find mature Oligodendrocytes in our sample set indicating that OPCs are also able to mature despite the glial scar.

To further investigate the plaque environment we traced astrocyte-derived factors during lesion evolution (summarized in Fig. 18). When looking at the results of astrocytic factors our findings suggest a very finely graduated and balanced system with different factors having to be present at particular time points in order to achieve successful repair. Normally those factors can act as either inhibiting or supporting OPCs. We suggest here that both functions are necessary and supportive in a way that – maybe also inhibition of OPCs entering a following step too early – is required for successful repair (17). Recent work of Anderson et al. showed that preventing glial scar formation or deleting chronic glial scars in severe spinal cord injury lesion in mice failed to result in a regrowth of axons. They even found out that a loss of the glial scar prevents stimulated axon regrowth. They therefore concluded that the glial scar rather aids than prevents axon regeneration (17,36).

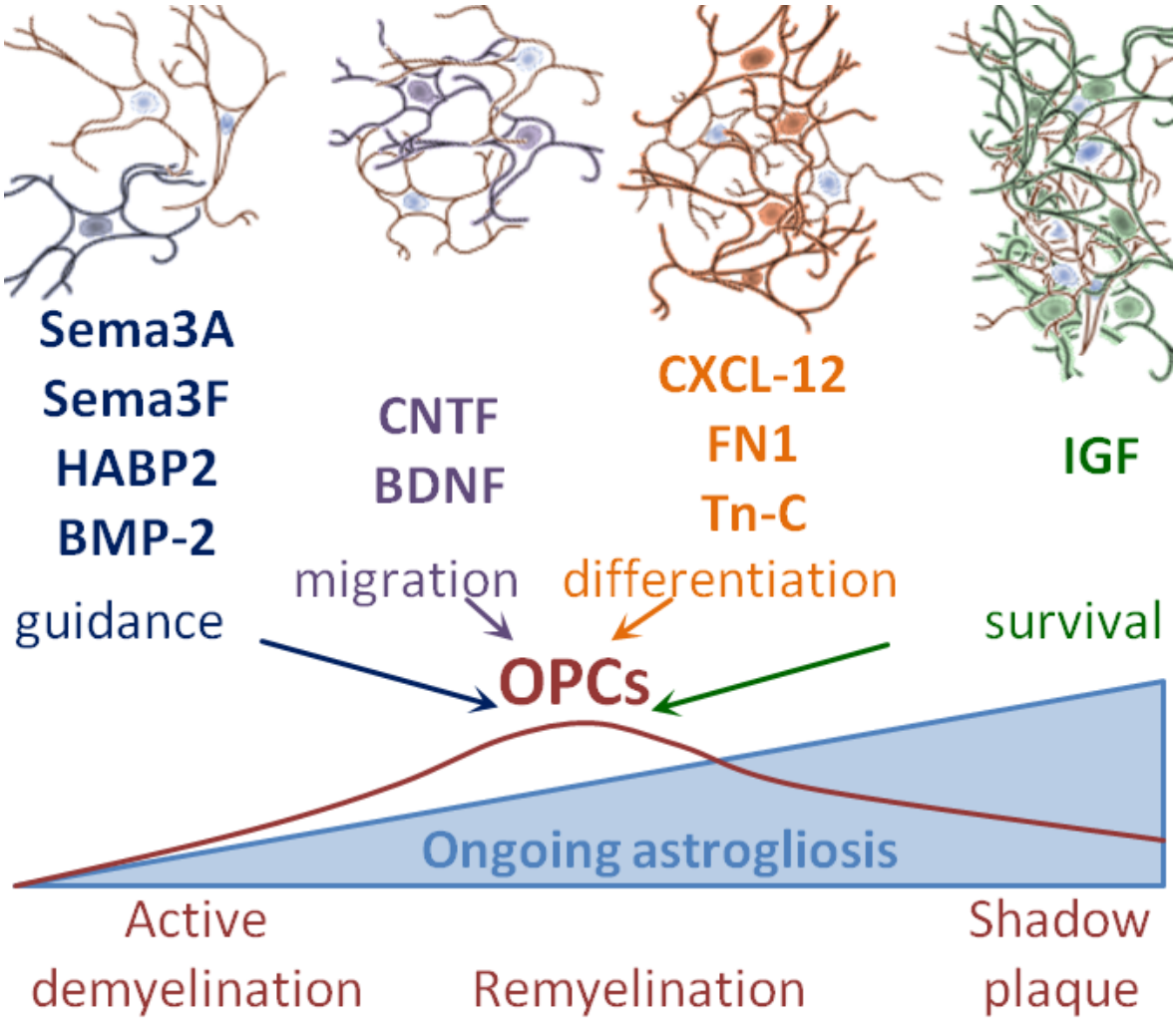

Figure 18: Overview of our main discussion on the glial scar and how astrocytes act. The light blue triangle indicates the ongoing astrogliosis during lesion evolution and the red line above indicates the OPC occurrence at the same time. This results in our main conclusion, that the glial scar does not prohibit remyelination. The factors expressed by astrocytes and supporting remyelination steps are written above the particular stages of oligodendrocytes from guidance to survival.

Beside the formation of a glial scar the very complex role of astrocytes is further characterized by their ability to exhibit different phenotypes and thereby to broaden their operational area. Neuroinflammation induces two different types of reactive astrocytes that were named "A1" and "A2" respectively (32). A1 astrocytes are induced by classically-activated neuroinflammatory microglia and were described as harmful by inhibiting OPC proliferation and differentiation while A2 astrocytes were suggested to be protective. In line with that we found A1 astrocytes mainly present in active lesions and the A2 phenotype during remyelination. Interestingly the distribution of the A1 phenotype also changed with the start of remyelination. During early remyelination A1 was detectable in a granular pattern spreading over the lesion. During later remyelination the A1

phenotype formed a ring surrounding the lesion which might act as a barrier to protect adjacent healthy tissue (17).

From our data we conclude that the formation of a glial scar after a demyelinating event does not *per se* prevent OPC survival, migration nor remyelination, presumably as long as a multitude of different cellular mediators are finely tuned in correct succession and dosage. This supports the new view of the glial scar not being a rigid border but rather provides a complex milieu of different factors influencing oligodendrocytes and presumably other cell types too. Contradicting findings from animal and cell culture studies indicate how complex and poorly understood the underlying signaling mechanisms still are. Regional differences between astrocytes, the activation state and the time point after destruction could very likely determine their overall function i.e. pro- or contra remyelination. Furthermore, in MS patients as well as in EAE there are different lesion types coexisting at each given timepoint. Since lesions are not rigid, strictly bordered structures, the cellular milieu can also be influenced through neighboring lesions. This dichotomy in astrocyte function makes these cells an interesting, though challenging target for new therapeutic strategies. A limitation of our work comes from the fact that we investigated experimental material only and additional systematic studies with human autopsy material of MS patients are necessary to validate our results for the human situation (17).

CLM: Features and novelty

With our CLM we are able to produce widespread cortical demyelination in MOG primed rats following cytokine injection through the implanted catheter. The cone-like shape of demyelination on day 1 seems consistent with the known physiological flow of interstitial fluid from cortical regions to the subarachnoid space (18,37). Similar to previous studies (25,38) cytokine injection alone did not lead to cortical demyelination which indicates that additional immunization against MOG or most likely other myelin components as well is required to induce cortical demyelination (18). The cortical demyelination on day 3 in the contralateral hemisphere was located directly underneath one of the anchor screws of our experimental setup. This could possible create a local “low-flow” area of cerebrospinal fluid similar to the proposed low flow area in the depth of the sulci of human brains leading to the typical band-like subpial cortical demyelination (18,39).

On day 15, where histological results showed peak disease with widespread cortical demyelination accompanied with microglial activation, we noted a marked slow, fatigued behavior in the rats and an increased startling reaction to normal sounds. In comparison

to EAE these are very mild symptoms (18). Interestingly, double-staining of GFAP and Caspase3 revealed mostly astrocytes being affected by apoptosis. Furthermore, this could be significant for overall tissue destruction as astrocytes are involved in trophic support and maintenance of tissue homeostasis (18,19,21). Astrocytes might try to ward the damage and die because of an overload. As a consequence neurons die as well because of the lack of trophic support. Still, remyelination does occur. In animals sacrificed on day 30 we already observed remyelination, which was accompanied with patches of subpial and intracortical still missing PLP. This appears consistent with human pathology of SPMS (18). After a second disease phase induced by another injection of cytokines a marked atrophy of the brain was obvious even macroscopically.

In comparison to other published models exhibiting cortical pathology (25,38,40) cortical involvement in our model spread far and persisted much longer – at least 30 days as compared to a few days until complete remyelination. One of course asks the question why. First, the previous models involved a single traumatic injection of cytokines, which *per se* disturbs the BBB and brings cellular infiltrates and blood components into the injection area. Second, with this method the amount of injectable liquid is restricted by anatomical limits. One might also speculate about a loss of cytokine through leakage into the blood when injected in an area with traumatically opened brain capillaries (18). We injected the cytokine mixture through a pre-implanted and healed catheter in an injection speed in line with the bulk flow rate of the brain interstitial fluid. This might avoid any mechanical trauma and the cytokines are transported with the interstitial fluid in the rat brain along their preferential pathways and finally ends up in the CSF around the brain convexity (18).

Our CLM offers a reproducible, widespread cortical demyelination with a peak on day 15 and resembles the key histological features of human SPMS cortical lesions. The extended presence of lesions as well as the possibility to induce a second demyelination phase are clear advantages over earlier versions summarized in figure 19. Symptoms in the animals are mild, thus a long-term observation and repeated demyelination phases appear ethically acceptable. The clinical symptoms in our animals correspond quite well to human MS patients who may despite widespread cortical demyelination exhibit only diffuse symptoms without motor disturbance (18). The implanted catheter furthermore offers the opportunity to inject prospective therapeutic agents or other substances directly in the cortical lesion area as well (18).

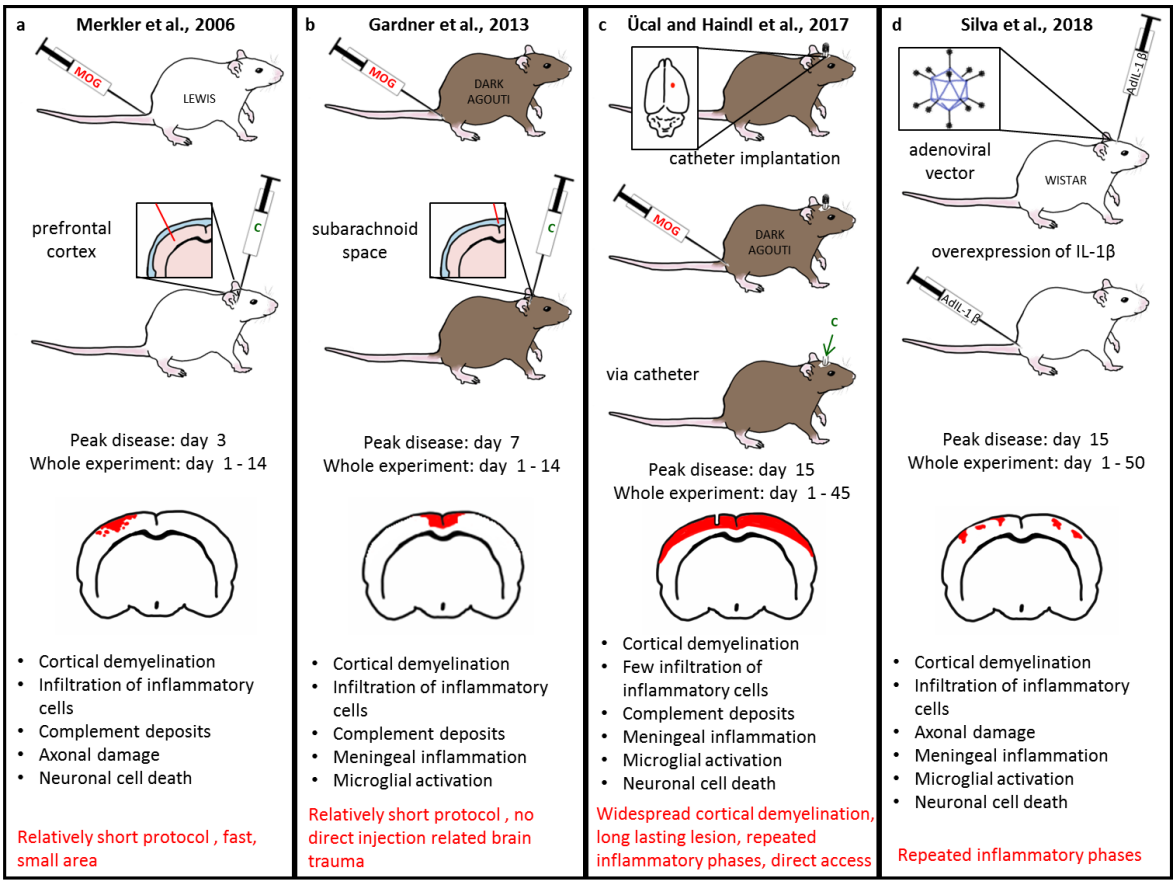

Figure 19: Comparison of so far available rat models reassembling cellular features of SPMS. The model used during this thesis is displayed in (c). In comparison to already existing models (a) and (b) and a new model (d) we could establish an animal model exhibiting long lasting widespread cortical demyelination. Cellular features of the models are listed under the brain schemes, advantages are listed in red and lesion width is indicated by the red mark on the brain scheme. Comparable with (d) we were also able to induce a second relapse. In (a) the model of Merkler et al. is represented. The protocol starts with the MOG immunization of Lewis rats. The pro-inflammatory cytokines are injected directly into the prefrontal cortex indicated by the inlet beside the second rat schema. Peak disease is on day 3 and cortical demyelination is fully remyelinated until day 14. The model is a fast protocol affecting a small cortex area but thereby reflecting good cellular comparability to human progressive MS. Panel (b) shows an overview of the animal model of Gardner et al. This model starts with the MOG immunization of DA rats and cytokines are injected into the subarachnoid space. Peak disease of cortical demyelination is on day 7 and lesions are largely resolved until day 14. Cortical lesions appear mainly round the injection area affecting both hemispheres. Again most of the cellular features know for the progressive MS in humans are reflected in this model and one big advantage is the avoidance of direct injection. Panel (c) describes the animal model of Ücal and Haindl et al. This model starts with the implantation of a catheter directly into the cortex. After a healing period DA rats are immunized with MOG and cytokines are given via the catheter. Peak disease is on day 15 and on day 30 some areas are already remyelinated. Via a second cytokine injection on day 30 another inflammatory phase can be induced lasting until day 45. In (d) the animal model of Silva et al is shown. This is the only model discussed here, using adenoviral vectors for an overexpression of IL-1beta. The experiment starts with a central injection of AdIL-1beta into the cortex of Wistar rats. After 21 days a repeated inflammatory stimulus is given by peripheral injection of AdIL-1beta (iv). Cortical demyelination peaked at day 15 which starts to resolve on day 30. Note, that the brain scheme does only show presumed lesion pattern since the authors did not give an overview

about the demyelinated hemisphere in their original work. Again this model shows several cellular features known to be present in human progressive disease phase. Reproduced from J. Neurol. Neuromed. 2018 with permission of the publisher.

CLM: Vitamin D acts as a potent antioxidant

The positive effect of vitD as an antioxidant on MS lesions on EAE was already confirmed in many cases (13,14). Nevertheless, so far there was no study available investigating the impact of vitD on cortical lesions in a CLM. In this thesis we could generate preliminary results for the first time and investigated at least a distinct part of the potential power of vitD. VitD seems to prevent demyelination, protected neurons and led to less microglia activation in our CLM when compared to animals fed with standard rodent food only. Furthermore there were more polyphenols in the serum of vitD supplemented rats detectable suggesting a better protection against oxidative stress in those animals. This was further confirmed by the investigation of TAC where only animals supplemented with vitD could reach a sufficient level. These are interesting findings especially because of the difference in cellular mechanisms between those two animal models and the RRMS and SPMS. To investigate this further and to be able to suggest an underlying mechanism further research with larger animal groups is necessary to further support these preliminary findings.

Conclusion: implication on neuroprotection and repair

Our results derived from the EAE model point towards astrocytes as crucial key regulators. Our main conclusion is that in this model shadow plaques can be glial scars at the same time, supporting the idea that the glial scar seems to be no rigid border but rather providing a complex milieu of different factors influencing oligodendrocytes and presumably other cell types too. This conclusion has a direct impact on the role of astrocytes involved in neuroprotection, with the glial scar not being the endpoint or even obstacle of repair processes (17). This is a very important finding for further research regarding neuroprotection and repair in brain diseases. The investigation of the complex cellular milieu could finally lead to therapeutic options intervening in one of those many signal transduction pathways. Attacks against astrocytes to prevent them from becoming reactive are most likely an imprudent approach.

Concerning our new cortical lesion model in summery we can say that a long lived and widespread demyelination selectively of the cerebral cortex can be produced through injection of pro-inflammatory cytokines via an implanted catheter in rats which were previously immunized with a low dose of MOG. The catheter is well tolerated by the rats, and except for some mild “slow” behavior between days 9-15 after cytokine injection there

were no obvious clinical symptoms in the experimental group. Spinal cord histology shows no changes in all groups. Control groups, with one component each of the experimental setup omitted, respectively, did not lead to myelin loss in the cortex. The induction of a second relapse through a second cytokine injection on (or after) day 30 is possible and due to the very mild symptoms even a long term observation seems ethically acceptable (18). This model offers many opportunities for investigating the complex cellular properties of cortical lesions and the close resemblance to human SPMS brain pathology could help further to investigate specific neuroprotective therapeutic agents.

The important role of astrocytes is not only suggested in EAE but also in our CLM model. These cells seem to be crucial key regulators in both. The idea that astrocytes exert multiple functions, both pro- and anti-inflammatory depending on their microenvironment and activation state became apparent in both investigated models. A very interesting observation in the EAE study was the astrocytic border suggested to protect healthy tissue and to avoid a spread of the damage. The white matter lesions in EAE differ clearly from healthy tissue, in contrast to those in the CLM where the cortical demyelination spreads in a rather diffuse way. One possible mechanism could be linked to astrocytes. There is no glial scar formed in the cortical lesions of CLM and the lesions seem to spread unhindered over the whole cortex. Furthermore the loss of predominantly astrocytes may cause a lack of trophic support leaving the brain more vulnerable in case of further attacks. In comparison the white matter lesions in EAE are strictly bordered from the healthy tissue so astrocytes might prevent a further spread of lesions. The new view of the glial scar offers additional opportunities to investigate remyelination facilitating factors in both – EAE and CLM – and how the balanced system, necessary for a remyelination facilitating environment, could be maintained.

Oxidative stress is indeed also an important factor in neuroprotection and repair. We could demonstrate that at least in our CLM model vitD has a protective effect and moderates the disease course, at least when the animals already grow up with a preventive high vitD supplementation. This leads to further ideas to investigate the exact mechanisms and how vitD could therapeutically be used for SPMS patients. If a vitD supplementation might have a similar protective effect at a later time, remains to be investigated.

Critical reflection on the content and methods

In our studies we are using animal models, which is associated with certain advantages – it allows us to trace cellular mechanisms very accurately over the full time course of lesion development. This would of course not have been possible with human tissue and

specimen. However, we are aware that results of an animal model can never be directly transferred to the human situation without considering limitations, as it is an artificial disease and not the human disease itself.

Using experimental EAE tissue allowed us to study basically one or few lesion stage in each animal at each time point. Genetic background and environmental influences are largely known and standardized. When investigating human tissue there are always many different lesion types aside each other and many environmental influences, which we do not know and cannot characterize. Thus, in case of for investigating basic cellular mechanisms animal models are indispensable but one has to keep in mind that animal models always can only reflect parts of the human situation (17).

Another limitation is the fact that EAE gives mainly rise of white matter lesions in the spinal cord and our CLM gives rise to cortical lesions only and produces no lesions in the spinal cord at all. Thus each of the animal models used can only represent one part of the human disease of MS.

All antibodies were tested carefully and there were always positive and negative controls stained within one run during IHC. However, it is important to know that there are always technical pitfalls in IHC and to ensure quality control we were aware of that and quantified all lesions very carefully. It is always desirable to combine many methods when investigating one research question. Due to our small team and limited access to other techniques we can only show the appropriate histological part of our work. This is another big goal for our future work, to broaden our methodical range due to embedding of MRI measurements, further serum analysis via SIMOA Quanterix, Fluorescence activated cell sorting (FACS) analysis and behavioral tests of the rats.

Novelty value

This dissertation resulted in two huge novel ideas. On the one hand it shows a new view of the glial scar and associated factors and how they might promote remyelination. This finding could lead to a rethinking of the role of astrocytes. It should prevent from hasty conclusions in targeting astrocytes and point to the very complex and manifold role of astrocytes. This could further even lead to new neuroprotective strategies in enhancing proper astrocytic factors in desired stages of repair. On the other hand this thesis introduces a new animal model reassembling cortical pathology of SPMS patients quite well. This model offers the great opportunity to test neuroprotective and repair facilitating substances directly in the lesions itself.

Furthermore, in this thesis for the first time the effects of vitD on cortical lesions were tested and indicates a beneficial, protective role of vitD, which could be further investigated for SPMS patients as well. The colorimetric tests for PPm and TAC were not yet tested on rats. Thus we had to modify the TAC setup and were pleased to found similar results to human studies in both tests. So also the accomplishment of those tests was never done before.

Outlook and suggestions for further work

Our first results regarding astrocytic involvement in disease mechanisms and repair consequently lead us to further research of astrocytes and their involvement in destruction and repair. The remyelination facilitating factors studied in EAE should further be investigated in our cortical lesions animal model as well. This could lead to a better understanding of the involvement of astrocytes in mechanisms of damage and repair. Furthermore we want to take a closer look at oxidative stress reactions and whether corresponding markers can help to understand the complex processes leading to degeneration and regeneration. VitD as an antioxidant seems to act protective in both, EAE and CLM. Both models could be used for further investigation of cellular mechanisms how vitD is acting and which supplementation protocol gives the best protective results. It is also a future goal of our research group to investigate new MRI sequences to detect cortical lesions. We are currently working on a B-cell depletion experiment to investigate whether new therapeutic approaches for RRMS could also work for the cellular situation of SPMS.

Bibliography

1. Lemus HN, Warrington AE, Rodriguez M. Multiple Sclerosis: Mechanisms of disease and strategies for myelin and axonal repair. Neurol Clin [Internet]. Elsevier Inc; 2018;36:1–11. Available from: https://doi.org/10.1016/j.ncl.2017.08.002

2. Haindl MT, Ücal M, Fazekas F, Hochmeister S. Overview of promising rat models for cortical lesion research- 2006 until now. J Neurol Neuromedicine. 2018;3(5):8–12.

3. Barnett MH, Mathey E, Kiernan MC, Pollard JD. Axonal damage in central and peripheral nervous system inflammatory demyelinating diseases: Common and divergent pathways of tissue damage. Curr Opin Neurol. 2016;29(3):213–21.

4. Thompson AJ, Baranzini SE, Geurts J, Hemmer B, Ciccarelli O. Multiple sclerosis. Lancet [Internet]. Elsevier Ltd; 2018;391:1622–36. Available from: http://dx.doi.org/10.1016/S0140-6736(18)30481-1

5. Hohlfeld R, Dornmair K, Meinl E, Wekerle H. The search for the target antigens of multiple sclerosis , part 1: autoreactive CD4 + T lymphocytes as pathogenic effectors and therapeutic targets. Lancet Neurol [Internet]. Elsevier Ltd; 2016;15(2):198–209. Available from: http://dx.doi.org/10.1016/S1474-4422(15)00334-8

6. Mallucci G, Peruzzotti-Jametti L, Bernstock JD, Pluchino S. The role of immune cells, glia and neurons in white and gray matter pathology in multiple sclerosis. Vols. 127–128, Progress in Neurobiology. 2015. p. 1–22.

7. Howell OW, Reeves CA, Nicholas R, Carassiti D, Radotra B, Gentleman SM, et al. Meningeal inflammation is widespread and linked to cortical pathology in multiple sclerosis. Brain. 2011;134:2755–71.

8. Domingues HS, Portugal CC, Socodato R, Relvas Joao B. Oligodendrocyte, astrocyte, and microglia crosstalk in myelin development, damage, and repair. Front cell Dev Biol. 2016;4(71).

9. Eshaghi A, Brownlee WJ, Altmann DR, Tur C, Cardoso MJ, Angelis F De, et al. Deep gray matter volume loss drives disability worsening in multiple sclerosis. Ann Neurol. 2018;83:210–22.

10. Hadžović-Džuvo A, Lepara O, Valjevac A, Avdagić N, Hasić S, Kiseljaković E, et al.

Serum total antioxidant capacity in patients with multiple sclerosis. Bosn J Basic Med Sci. 2011;11(1):33–6.

11. Solleiro-Villavicencio H, Rivas-Arancibia S. Effect of chronic oxidative stress on neuroinflammatory response mediated by CD4+T cells in neurodegenerative diseases. Front Cell Neurosci [Internet]. 2018;12(114). Available from: http://journal.frontiersin.org/article/10.3389/fncel.2018.00114/full

12. Bhullar KS, Rupasinghe HPV. Polyphenols: Multipotent therapeutic agents in neurodegenerative diseases. Oxid Med Cell Longev. 2013;2013:1–18.

13. Sintzel MB, Rametta M, Reder AT. Vitamin D and Multiple Sclerosis: A Comprehensive Review. Neurol Ther [Internet]. Springer Healthcare; 2018;7(1):59–85. Available from: https://doi.org/10.1007/s40120-017-0086-4

14. Adzemovic MZ, Zeitelhofer M, Hochmeister S, Gustafsson SA, Jagodic M. Efficacy of vitamin D in treating multiple sclerosis-like neuroinflammation depends on developmental stage. Exp Neurol. 2013;249:39–48.

15. Dobson R, Giovannoni G. Multiple sclerosis – a review. Eur J Neurol. 2019;26:27–40.

16. Plemel JR, Liu W, Yong VW. Remyelination therapies: multiple sclerosis. Nat Rev Drug Discov. 2017;16:1–18.

17. Haindl MT, Köck U, Zeitelhofer-Adzemovic M, Fazekas F, Hochmeister S. The formation of a glial scar does not prohibit remyelination in an animal model of multiple sclerosis. Glia [Internet]. 2019;67(3):467–81. Available from: http://doi.wiley.com/10.1002/glia.23556

18. Ücal M, Haindl MT, Adzemovic MZ, Strasser J, Theisl L, Zeitelhofer M, et al. Widespread cortical demyelination of both hemispheres can be induced by injection of pro-inflammatory cytokines via an implanted catheter in the cortex of MOG-immunized rats. Exp Neurol [Internet]. Elsevier Inc.; 2017;294:32–44. Available from: http://www.ncbi.nlm.nih.gov/pubmed/28457906%0Ahttp://linkinghub.elsevier.com/retrieve/pii/S0014488617301073

19. Ludwin SK, Rao VT, Moore CS, Antel JP. Astrocytes in multiple sclerosis. Mult Scler J [Internet]. 2016;22(9):1114–24. Available from: http://msj.sagepub.com/cgi/doi/10.1177/1352458516643396%5Cnhttp://www.ncbi.n

lm.nih.gov/pubmed/27207458

20. Nair A, Frederick TJ, Miller SD. Astrocytes in multiple sclerosis: A product of their environment. Cell Mol Life Sci. 2008;65(17):2702–20.

21. Sofroniew M V., Vinters H V. Astrocytes: Biology and pathology. Acta Neuropathol. 2010;119(1):7–35.

22. Brambilla R, Morton PD, Ashbaugh JJ, Karmally S, Lambertsen KL, Bethea JR. Astrocytes play a key role in EAE pathophysiology by orchestrating in the CNS the inflammatory response of resident and peripheral immune cells and by suppressing remyelination. Glia. 2014;62(3):452–67.

23. Patrikios P, Stadelmann C, Kutzelnigg A, Rauschka H, Schmidbauer M, Laursen H, et al. Remyelination is extensive in a subset of multiple sclerosis patients. Brain. 2006;129(12):3165–72.

24. Kutzelnigg A, Lucchinetti CF, Stadelmann C, Brück W, Rauschka H, Bergmann M, et al. Cortical demyelination and diffuse white matter injury in multiple sclerosis. Brain. 2005;128(11):2705–12.

25. Gardner C, Magliozzi R, Durrenberger PF, Howell OW, Rundle J, Reynolds R. Cortical grey matter demyelination can be induced by elevated pro-inflammatory cytokines in the subarachnoid space of MOG-immunized rats. Brain. 2013;136(12):3596–608.

26. Ontaneda D, Thompson AJ, Fox RJ, Cohen JA. Progressive multiple sclerosis: prospects for disease therapy, repair, and restoration of function. Lancet [Internet]. Elsevier Ltd; 2017;389:1357–66. Available from: http://dx.doi.org/10.1016/S0140-6736(16)31320-4

27. Stankoff B, Jadasz JJ, Hartung HP, Küry P, Zalc B, Lubetzki C. Repair strategies for multiple sclerosis: Challenges, achievements and perspectives. Curr Opin Neurol. 2016;29(3):286–92.

28. Cummings J. Disease modification and neuroprotection in neurodegenerative disorders. Transl Neurodegener. Translational Neurodegeneration; 2017;6(25).

29. Hochmeister S, Romauch M, Bauer J, Seifert-Held T, Weissert R, Linington C, et al. Re-expression of N-cadherin in remyelinating lesions of experimental inflammatory demyelination. Exp Neurol [Internet]. Elsevier Inc.; 2012;237(1):70–7. Available

from: http://dx.doi.org/10.1016/j.expneurol.2012.06.010

30. Seifert T, Bauer J, Weissert R, Fazekas F, Storch MK. Notch1 and its ligand Jagged1 are present in remyelination in a T-cell- and antibody-mediated model of inflammatory demyelination. Acta Neuropathol. 2007;113:195–203.

31. Storch MK, Bauer J, Linington C, Olsson T, Weissert R, Lassmann H. Cortical demyelination can be modeled in specific rat models of autoimmune encephalomyelitis and is major histocompatability complex (MHC) haplotype-related. J Neuropathol Exp Neurol. 2006;65(12):1137–42.

32. Liddelow SA, Guttenplan KA, Clarke LE, Bennett FC, Bohlen CJ, Schirmer L, et al. Neurotoxic reactinve astroctes are induced by activated microglia. Nature. 2017;541(7638):481–7.

33. Zelzer S, Tatzber F, Herrmann M, Wonisch W, Rinnerhofer S, Kundi M, et al. Work intensity, low-grade inflammation, and oxidative status: a comparison between office and slaughterhouse workers. Oxid Med Cell Longev [Internet]. 2018;2018:1–7. Available from: https://www.hindawi.com/journals/omcl/2018/2737563/

34. Tatzber F, Griebenow S, Wonisch W, Winkler R. Dual method for the determination of peroxidase activity and total peroxides-iodide leads to a significant increase of peroxidase activity in human sera. Anal Biochem. 2003;316(2):147–53.

35. Hagemeier K, Brück W, Kuhlmann T. Multiple sclerosis - remyelination failure as a cause of disease progression. Histol Histopathol. 2012;27(3):277–87.

36. Anderson MA, Burda JE, Ren Y, Ao Y, Coppola G, Khakh BS, et al. Astrocyte scar formation aids CNS axon regeneration. Nature. 2016;532(7598):195–200.

37. Abbott NJ. Evidence for bulk flow of brain interstitial fluid : significance for physiology and pathology. 2004;45:545–52.

38. Merkler D, Ernsting T, Kerschensteiner M, Brück W, Stadelmann C. A new focal EAE model of cortical demyelination: Multiple sclerosis-like lesions with rapid resolution of inflammation and extensive remyelination. Brain. 2006;129(8):1972–83.

39. Kutzelnigg A, Lassmann H. Cortical demyelination in multiple sclerosis : A substrate for cognitive deficits ? 2006;245:123–6.

40. Silva BA, Leal MC, Farías MI, Avalos JC, Besada CH, Pitossi FJ, et al. A new focal

model resembling features of cortical pathology of the progressive forms of multiple sclerosis: Influence of innate immunity. Brain Behav Immun [Internet]. Elsevier Inc.; 2018;69:515–31. Available from: https://doi.org/10.1016/j.bbi.2018.01.010

Appendix

Supplementary table 1: The following antibodies have been used:

Antibody		Host	AB-ID	Dilution	Company	Catalog number
BDNF	Anti-BDNF antibody [EPR1292], monoclonal	rabbit	AB_ 10862052	1:1000	Abcam	ab108319
BMP-2	Polyclonal BMP-2 antibody	rabbit	AB_ 10641999	1:100	PTG/ Protein-tech	18933-1-AP
C3d	Complement C3d antibody	goat		1:1000	R & D Systems	AF2655
CNTF	Anti-CNTF antibody, polyclonal	rabbit		1:1000	Abcam	ab190985
CXCL-12	SDF-1 (C-19), polyclonal	goat	AB_ 2088173	1:300	Santa Cruz	sc-6193
ED1	Anti-rat-CD68	mouse	AB_ 2291300	1:1000	Serotec	MCA341R
FGF-2	Anti-FGF basic antibody, polyclonal	rabbit	AB_ 306833	1:5000	Abcam	ab8880
FN1	Polyclonal Fibronectin atnibody	rabbit	AB_ 2105691	1:1000	PTG/ Protein-tech	15613-1-AP
GFAP	GFAP (Glial Fibrillary Acidic Protein) Ab-6 (Clone ASTRO6), monoclonal	mouse	AB_ 62808	1:100	Thermo Scientific	MS-1376-P
HABP2	Polyclonal HABP2 antibody	rabbit	AB_ 10640521	1:500	PTG/ Protein-tech	12863-1-AP
IGF	Anti-IGF1 Receptor antibody, polyclonal	rabbit	AB_ 11155487	1:500	Abcam	ab131476
IL-6	Anti-IL6 antibody,	rabbit	AB_	1:1000	Abcam	ab6672

	polyclonal		2127460			
Nestin	Mouse monoclonal Nestin antibody	mouse		1:1000	PTG/ Protein-tech	66259-1-Ig
NOGO	Polyclonal RTN4/NOGO antibody	rabbit		1:50	PTG/ Protein-tech	10950-1-AP
PLP	Anti-myelin Proteolipid Protein antibody	mouse	AB_ 2237198	1:1000	Serotec	MCA839G
S100 A10	Anti-S100A10 antibody	rabbit		1:1000	Abcam	ab187201
Sema 3A	Anti-Semaphorin 3A antibody, polyclonal	rabbit	AB_ 447408	1:500	Abcam	ab23393
Sema 3F	Sema3F/Semaphorin 3F antibody, polyclonal	rabbit	AB_ 10853039	1:500	Bioss	bs-1122R
Sec. antib. anti-mouse	anti-mouse IgG biotinylated species specific whole antibody from sheep	sheep		1:200	GE Health-care	RPN1001V1
Tn-C	Tenascin C polyclonal antibody	rabbit	AB_ 10855943	1:200	Bioss	bs-1039R
Vimentin	Polyclonal Vimentin antibody	rabbit	AB_ 2273020	1:1000	PTG/ Protein-tech	10366-1-AP

Supplementary table 2: The following groups of animals have been used for the CLM

Experiment	Number of used rats
Dose finding experiment (immunization)	15
Catheter control (sacrificed 4 weeks after implantation)	5
Catheter implantation + MOG Immunization	6
VitD supplemented controls	5
Day 1	5
Day 1 cytokine only	2
Day 1 immunized and sterile PBS injection intracortically	2
Day 3	5
Day 3 cytokine only	2
Day 3 immunized and PBS	2
Day 15	6
Day 15 vitD supplemented	7
Day 15 cytokine only	2
Day 15 immunized and PBS	2
Day 30	5
Day 30 vitD supplemented	5
Day 30 immunized and PBS	2
Day 15 2nd cytokine injection	4
Day 15 2nd cytokine injection vitD supplemented	7

In total 65 animals were used for establishing the model and 24 animals were supplemented with vitD which results in a total number of 89 animals.

Supplementary table 3: Median and percentile of GFAP, PLP and NOGO quantification.

GFAP			
	Median	**25. Percentile**	**75 Percentile**
NAWM	102.00	98.00	139.00
A	194.00	133.00	266.00
IA/ER	843.50	620.75	1120.25
ER/LR	1600.00	1302.25	1793.00
LR/SP	2088.50	1838.00	2366.75
SP	4498.00	4133.50	5131.50
PLP			
	Median	**25. Percentile**	**75 Percentile**
NAWM	587.00	563.00	701.50
A	20.00	13.50	32.50
IA/ER	1479.00	1083.25	1757.50
ER/LR	726.50	491.00	964.50
LR/SP	696.00	491.50	854.50
SP	614.00	450.00	890.00
NOGO			
	Median	**25. Percentile**	**75 Percentile**
NAWM	307.50	256.00	368.00
A	66.50	43.50	82.00
IA/ER	476.00	394.00	502.00
ER/LR	645.50	575.75	686.00
LR/SP	496.50	473.50	509.50
SP	325.00	276.00	376.25